To the Graduate Council:

I am submitting herewith a dissertation written by Gregory Vonzell Murphy entitled "Robust LQG/LTR Control System Design for a Low-Pressure Feedwater Heater Train with Time Delay." I have examined the final copy of this dissertation for form and content and recommend that it be accepted in partial fulfillment of the requirements for the degree of Doctor of Philosophy, with a major in Electrical Engineering.

J. M. Bailey

J. M. Bailey, Major Professor

We have read this dissertation and recommend its acceptance:

A. O. Bishop Jr.

A. O. Bishop, Jr.

J. M. Googe

J. M. Googe

J. S. Lawler

J. S. Lawler

BR Upadhyaya

B. R. Upadhyaya

Accepted for the Council:

C W Minkel

Vice Provost
and Dean of The Graduate School

ROBUST LQG/LTR CONTROL SYSTEM DESIGN FOR A LOW-PRESSURE FEEDWATER HEATER TRAIN WITH TIME DELAY

A Dissertation

Presented for the

Doctor of Philosophy

Degree

The University of Tennessee, Knoxville

Gregory Vonzell Murphy

August 1990

Dedicated to my son Jared for his honest curiosity and energetic exploits, which are always delightful and refreshing.

ACKNOWLEDGMENTS

First, I would like to thank my dissertation advisor, Professor J. M. Bailey. Without his guidance and support this research would not have been possible.

Next, I am grateful to my committee members, Dr. Asa O. Bishop, Jr., Dr. Joseph M. Googe, Dr. Jack S. Lawler, and Dr. Belle R. Upadhyaya for their experience and helpful comments during this research.

In addition, I would like to thank my colleagues at the University of Tennessee for their friendship and for many enlightening philosophical and academic conversations. The experience and knowledge that I gain from our association is immeasurable. I am grateful to Ali Alouani, Frank Chow, Kin Fung, and Jalel Zrida.

I wish to thank James Pippin, Director of the Minority Engineering Scholarship Program (MESP), and his staff, Dorothy Mynatt and Christopher Randolph (assistant director), for their support, encouragement, help, and cheerful attitude during the course of my academic studies.

I am grateful to LaWanda Klobe for editing this work and for many helpful suggestions to improve its quality. I also wish to thank Vicky Rolfe for keying this document with the utmost efficiency and accuracy. Thanks also to Kimberly D. Daniels for the computer production of diagrams and tables, which truly improved this document. I greatly appreciate the response of LaWanda, Vicky, Kimberly, and the staff of the Instrumentation and Controls Division Publications Office to complete this job in the face of rapidly approaching deadlines.

Finally, I would like to thank my Father, Booker T. Murphy, my mother Emma D. Murphy (deceased), my great uncle and aunt, John and Mary Walls, my brother and sisters and other relatives and friends for their support through my endless academic years. Last, I would like to thank my cousin Jessie A. Murphy (deceased) whose energy, intellect, and wisdom over the years I will always remember and cherish.

This research work was supported by and performed for the Advanced Controls Program (ACP) of the Oak Ridge National Laboratory, operated by Martin Marietta Energy systems, Inc., for the U.S. Department of Energy under
Contract No. DE-AC05-84OR21400.

ABSTRACT

In this dissertation a systematic control design methodology is introduced for multiple input/multiple output (MIMO) systems with time delay. The methodology is applied to plants with right half-plane zeros. This methodology allows the control engineer to design and analyze MIMO systems in a manner analogous to single input/single output (SISO) systems.

This methodology uses a minimum phase control system design technique, LQG/LTR, in obtaining a stable control system with some limitations on achievable performance. This methodology incorporates the computation, both graphically and analytically, of the maximum allowable time delay before instability occurs in the control system. Conservative results are seen to exist for the analytical results and are verified by time domain analysis.

This methodology provides a useful approach to the design of process control systems with time delay that allows many of the intuitive concepts of classical control SISO systems to be identifiable for the MIMO system.

TABLE OF CONTENTS

TABLE OF CONTENTS (Continued)

LIST OF FIGURES

LIST OF FIGURES (Continued)

Figure | Page

LIST OF TABLES

CHAPTER 1

INTRODUCTION

1.1 PROBLEM

In the nuclear power industry reliable control of nuclear reactors is of great concern because of the possible detrimental effects of an accident on the environment and the public. Reliable control of a nuclear reactor also minimizes shutdowns, which can cost on the order of millions of dollars if they continue for a prolonged period of time. One major source of nuclear power plant shutdown is the feedwater control system. In the nuclear power industry, feedwater control systems have been responsible for three U.S. plant shutdowns per year for BWRs (boiling water reactors) [1]. The Northern States Power (NSP) Company established an overall system design goal of 10 years without a control-system-related reactor scram. Criteria such as this are resulting in a search for modern control system design strategies to apply to control of the feedwater component of a nuclear reactor.

The remainder of this chapter discusses previous control system design techniques and advances in modern control theory that could assist in solving this problem.

1.2 PREVIOUS WORK AND RESULTS

Most applications of modern control techniques to process control have appeared in the form of optimal control strategies, as noted in the case studies given in Ref. 2. These optimal control strategies were in the form of full-state feedback control with and without state estimation [linear-quadratic regulator (LQR)]. The regulator problem, coupled with a state estimation problem, was shown by Doyle [3] not to have desirable robustness properties. Doyle and Stein [4] proposed a multivariable robust design philosophy known as LQG/LTR (linear-quadratic-Gaussian with loop transfer recovery) to eliminate the shortcomings of the LQR and LQG design techniques. The LQG/LTR design technique has been applied to control submersible vehicles, engine speed, helicopters, ship steering, and large, flexible space structures. Considering the diversity of applications, there appears to be a significant void when it comes to applications in process control.

The LQG/LTR method requires the plant to be minimum phase, which cannot be guaranteed in a plant process. Typically nonminimum phase conditions in a plant process are due to time delay. The LQG/LTR design procedure offers no guarantees when a nonminimum phase plant is used [5].

The LQG/LTR synthesis method for minimum phase plants is an excellent method for achieving desired loop shapes and maximum robustness properties in the design of feedback control systems. First, a Kalman filter (or alternatively, a full-state LQ feedback regulator) with desired loop transfer properties is designed. Then a sequence of LQ feedback regulator gains (or alternatively, Kalman filter gains) approaching an ideal limit is selected to recover the loop shape of the Kalman filter (or alternatively, an LQ regulator) at the plant output (or alternatively, plant input) of the LQG compensator.

The time domain solution to an optimal LQR with time delays in the state and control was proposed in Ref. 6. However, this method for typical control system design appears mathematically formidable and does not yield the frequency-domain design interpretation generally expected by control engineers to determine system robustness.

Recent literature [7,8], reports efforts that have been made to analyze in the frequency domain the effects of nonminimum phase poles and zeros on multiple-input/multiple-output (MIMO) control systems performance and sensitivity, regardless of the design method. The results show that for a finite number of right half-plane (rhp) zeros in a MIMO control system, the performance limitations are analogous to those of a single-input/single-output (SISO) system.

It appears that relaxing the criterion of solving a control problem for an exact time delay makes available a viable design and analysis procedure using the LQG/LTR design technique. The idea of settling for a finite approximation of time delay in the control problem eliminates the true essence of the problem for some control engineers. This, however, is not true, but it does make available additional analysis and design tools and minimizes the mathematical burden of the control system design. In Ref. 9 it is stated that MIMO control systems using a Padé approximation of time delay are indistinguishable from those using controllers based on irrational models. Thus the design of a LQG/LTR controller for process control using an approximation of time delay resulting in a stable controller with some limitations in achievable performance is a viable and unexplored alternative for process control.

The intent of this work is to develop well-understood procedures for design and analysis of process controls with time delay.

1.3 NEW DEVELOPMENTS

An LQG/LTR control system design is formulated for a feedwater heater train with time delay. This approach involves factoring the feedwater heater train plant into nonminimum and minimum phase components to allow the design of a robust controller for the minimum phase component of the plant using the LQG/LTR technique (minimum phase method).

The nonminimum phase component takes the form of an all-pass filter containing the rhp zeroes of the first-order approximation of the time delay component. Using this nonminimum phase all-pass filter, certain singular-value multiplicative error bounds can be established to obtain a stable control system when using the LQG/LTR design technique on the minimum phase component of the plant.

New analysis methods using singular values is integrated into the conventional singular-value performance and stability robustness analysis procedure. These new analysis methods allow computation of the maximum allowable time delay before instability occurs for both SISO and MIMO control systems.

CHAPTER 2

MATHEMATICS AND CONTROL BACKGROUND

The use of matrix algebra is very important in the study of MIMO control system design methods. Some MIMO control system design methods use matrix algebra to decouple the system so that the plant matrix transfer function consists only of individual decoupled transfer functions, each represented conventionally as the ratio of two polynomials. This simplification then allows the use of conventional methods such as the Bode plot, Nyquist plot, and Nichols chart as a means of designing a controller for each loop of the MIMO plant. The LQG/LTR control system design method, however, does not require decoupling of the plant but rather preserves the coupling between the individual loops of the MIMO plant. Each step of the LQG/LTR design technique therefore requires the use of some matrix algebra, vector and matrix norms, and singular values during the control system design procedure. For instance, matrix algebra is used to derive a suitable representation of the closed-loop system for stability and robustness analysis as discussed in Chapter 3. Matrix norms and singular values are used to examine the matrix magnitude of the MIMO transfer function. The matrix magnitude or singular values of a system allows preservation of the coupling between the various loops of the MIMO control system. The use of singular values is essential in the synthesis of the frequency-domain LQG/LTR design technique, which is described in Chapter 6.

The concepts of controllability, observability, stabilizability, and detectability are very important in applying the LQG/LTR design procedure discussed in this work. The lack of stabilizability and detectability can eliminate the use of the LQG/LTR procedure as a control system design strategy. It is therefore important that these concepts be well understood.

The purpose of this chapter is to present some background material in mathematics and control systems that has proved to be very useful in deriving the relationship and the procedures and analysis required to implement the control system design procedure presented in this work.

2.1 MATRIX IDENTITIES AND PROPERTIES

Some properties of matrix transpose are as follows [10]. The transpose of the sum of two matrices is the sum of the transposed matrices;

$$(\mathbf{A} + \mathbf{B})^T = \mathbf{A}^T + \mathbf{B}^T \ . \tag{2.1}$$

The transpose of the transpose of a given matrix is identical with the given matrix;

$$(\mathbf{A}^T)^T = \mathbf{A} \ . \tag{2.2}$$

The transpose of the product of two matrices is the product of the transpose of the individual matrices in reverse order;

$$(\mathbf{AB})^T = \mathbf{B}^T\mathbf{A}^T \ . \tag{2.3}$$

The transpose of a symmetric matrix is that matrix;

$$\mathbf{A}^T = \mathbf{A} \ . \tag{2.4}$$

The Hermitian transpose of a matrix is the complex conjugate transpose of the matrix;

$$\mathbf{A}^H = \mathbf{A}^{*T} \ , \tag{2.5}$$

where * indicates complex conjugate.

Classification of different matrix types [10,11]:

A matrix **B** is real if all of its elements are real.

A matrix **B** is imaginary if all of its elements are imaginary.

A matrix **B** is Hermitian if it satisfies the following:

$$\mathbf{B}^H = \mathbf{B} \ . \tag{2.6}$$

A matrix **B** is positive definite if all of the eigenvalues of **B** are greater than zero;

$$\lambda_i(\mathbf{B}) > 0 \quad \forall\, i \ . \tag{2.7}$$

A matrix **B** is positive semidefinite if the eigenvalues of **B** are greater than zero and at least one eigenvalue is zero;

$$\lambda_i(\mathbf{B}) \geq 0 \ \forall\, i \ , \tag{2.8}$$

and

$$\lambda_{i_1}(\mathbf{B}) = 0 \text{ for some } i_1 \in \{1,2,\ldots,n\} \ . \tag{2.9}$$

A matrix **B** is negative definite if all of the eigenvalues of **B** are negative;

$$\lambda_i(\mathbf{B}) < 0 \ \forall\, i \ . \tag{2.10}$$

A matrix **B** is negative semidefinite if all of the eigenvalues of **B** are nonpositive and at least one eigenvalue is zero;

$$\lambda_i(\mathbf{B}) \leq 0 \ \forall\, i \ , \tag{2.11}$$

and

$$\lambda_{i_1}(\mathbf{B}) = 0 \text{ for some } i_1 \in \{1,2,\ldots,n\} \ . \tag{2.12}$$

Some properties of matrix multiplication and inverses [12–14]:

$$\mathbf{AB} \neq \mathbf{BA} \ . \tag{2.13}$$

$$(\mathbf{AB})^H = \mathbf{B}^H\mathbf{A}^H \ . \tag{2.14}$$

$$\mathbf{A}(\mathbf{BC}) = (\mathbf{AB})\mathbf{C} \ . \tag{2.15}$$

$$\mathbf{A}(\mathbf{B} + \mathbf{C}) = \mathbf{AB} + \mathbf{AC} \ . \tag{2.16}$$

$$\mathbf{AB} = 0 \text{ does not imply that } \mathbf{A} = 0 \text{ or } \mathbf{B} = 0 \ . \tag{2.17}$$

$$\mathbf{AB} = \mathbf{AC} \text{ does not imply that } \mathbf{B} = \mathbf{C} \ . \tag{2.18}$$

$$\mathbf{AB}(\mathbf{I} + \mathbf{AB})^{-1} = (\mathbf{I} + \mathbf{AB})^{-1}\mathbf{AB} \ . \tag{2.19}$$

$$\mathbf{AB}(\mathbf{I} + \mathbf{AB})^{-1} = [\mathbf{I} + (\mathbf{AB})^{-1}]^{-1} \ . \tag{2.20}$$

The right pseudoinverse of a matrix **A** is defined as

$$\mathbf{A}^R = \mathbf{A}^T(\mathbf{AA}^T)^{-1} \ . \tag{2.21}$$

The left pseudoinverse of a matrix **A** is defined as

$$\mathbf{A}^L = (\mathbf{A}^T\mathbf{A})^{-1}\mathbf{A}^T \ . \tag{2.22}$$

2.2 EIGENVALUES AND EIGENVECTORS

Assume that the linear time invariant (LTI) system is defined as

$$\dot{x} = \mathbf{A}x + \mathbf{B}u \quad , \tag{2.23}$$

and

$$y = \mathbf{C}x \quad , \tag{2.24}$$

where $x \in R^n$, $u \in R^p$, and $y \in R^p$. The letters n and p are, respectively, the dimensions of the states and the input and output where the inputs and outputs are the same dimensions.

The eigenvalues of **A** are defined as $\lambda_i (i = 1,2,...,n)$. The left eigenvector v_i^T of **A** is defined such that is satisfies

$$v_i^T(\mathbf{A} - \lambda_i \mathbf{I}) = 0 \quad , \tag{2.25}$$

and the right eigenvector u_i of **A** is defined to satisfy

$$(\mathbf{A} - \lambda_i \mathbf{I})u_i = 0 \ . \tag{2.26}$$

Note that for each left or right eigenvector there corresponds an eigenvalue λ_i, which is already defined prior to the solution of the eigenvector. A characteristic of the left and right eigenvectors is the orthogonal relationship that exists between them. The orthogonal relationship is defined as

$$v_i^T u_i = \begin{cases} 1 & \text{for } i = j \\ 0 & \text{for } i \neq j \end{cases} \quad . \tag{2.27}$$

Considering that the **A** matrix has distinct eigenvalues, **A** can be decomposed as follows:

$$\mathbf{A} = T \Lambda T^{-1} \quad , \tag{2.28}$$

where Λ is a diagonal matrix containing the eigenvalues, $T = [u_1, u_2, u_3,...,u_n]$, and $T^{-1} = [v_1^T, v_2^T, v_3^T,...,v_n^T]^T$. The representation of **A** given in Eq. (2.28) is called the eigenvector decomposition [10,15].

2.3 VECTOR NORMS

The size of a vector x is described by the concept of norm, which most engineers tend to associate with length. Before the concept of vector norm is formally defined, let us review the concept of inner product. The inner product of the complex vectors $x = [x_1, x_2,...,x_n]^T$ and $y = [y_1, y_2,...,y_n]^T$ is defined as

$$<x,y> = (x)^H y = x_1^* y_1 + x_2^* y_2 + ... + x_n^* y_n = <y,x> \quad , \tag{2.29}$$

where $(\ )^H$ indicates the Hermitian transpose and $(\ )^*$ defines the complex conjugate. The Hermitian transpose is defined as the complex conjugate transpose of the indicated vector or matrix.

The definitions of the 1, 2 (Euclidean norm), ∞ vector norms are defined respectively as

$$\|x\|_1 = |x_1| + |x_2| + ... + |x_n| \quad , \tag{2.30}$$

$$\|x\|_2 = (<x, x>)^{1/2} = (x_1^* x_1 + x_2^* x_2 + ... + x_n^* x_n)^{1/2} \quad , \tag{2.31}$$

and

$$\|x\|_\infty = \max_i |x_i| \quad . \tag{2.32}$$

2.4 MATRIX NORMS AND SINGULAR VALUES

Now the matrix norms of $\|\mathbf{A}\|_1$, $\|\mathbf{A}\|_2$, and $\|\mathbf{A}\|_\infty$ will be defined for the $m \times n$ matrix **A**. The matrix **A** defines a linear transformation from the vector space V, called the domain to a vector space W, which is called the range. Thus the linear transformation

$$\mathbf{A}(x) = \mathbf{A}x \tag{2.33}$$

transforms a vector x in $V \in C^n$ into a vector $\mathbf{A}(x)$ in $W \in C^m$. The matrix norms of $\|\mathbf{A}\|_1$, $\|\mathbf{A}\|_2$, and $\|\mathbf{A}\|_\infty$ are respectively defined as

$$\|\mathbf{A}\|_1 = \max_{x \neq 0} \frac{\|\mathbf{A}x\|_1}{\|x\|_1} \quad , \tag{2.34}$$

$$\|\mathbf{A}\|_2 = \max_{x \neq 0} \frac{\|\mathbf{A}x\|_2}{\|x\|_2} = \ell_2 \text{ norm} \quad , \tag{2.35}$$

and

$$\|\mathbf{A}\|_\infty = \max_{x \neq 0} \frac{\|\mathbf{A}x\|_\infty}{\|x\|_\infty} \quad . \tag{2.36}$$

Since the ℓ_2 norm is a useful tool in control system analysis, further insight into its definition will now be given. The ℓ_2 norm of Eq. (2.35) can be written as

$$\|\mathbf{A}\|_2 = \max_i [\lambda_i(\mathbf{A}^H\mathbf{A})]^{1/2}, \; i = 1,2,\ldots,n \tag{2.37}$$

$$= \max_i [\lambda_i(\mathbf{A}\mathbf{A}^H)]^{1/2}, \; i = 1,2,\ldots,n \quad . \tag{2.38}$$

The matrices $\mathbf{A}^H\mathbf{A}$ and $\mathbf{A}\mathbf{A}^H$ are Hermitian and positive semidefinite. The eigenvalues of these matrices are real and nonnegative.

Now let us define the singular value of a complex matrix $A \in C^{n \times n}$:

$$\sigma_i(A) = [\lambda_i(A^H A)]^{1/2} = [\lambda_i(AA^H)]^{1/2} \geq 0,\ i = 1,2,\ldots,n \quad . \tag{2.39}$$

More properties of singular values [16–18]:

$$\bar{\sigma}(A) = \frac{1}{\underline{\sigma}(A^{-1})} \quad . \tag{2.40}$$

$$\bar{\sigma}(A + P) \leq \bar{\sigma}(A) + \bar{\sigma}(P) \quad . \tag{2.41}$$

$$\bar{\sigma}(AP) \leq \bar{\sigma}(A)\bar{\sigma}(P) \quad . \tag{2.42}$$

$$\underline{\sigma}(A)\underline{\sigma}(P) \leq \underline{\sigma}(AP) \quad . \tag{2.43}$$

$$\underline{\sigma}(A) - \bar{\sigma}(P) \leq \underline{\sigma}(A + P) \leq \underline{\sigma}(A) + \bar{\sigma}(P) \quad . \tag{2.44}$$

where $\bar{\sigma}$ is maximum singular value $\underline{\sigma}$ is minimum singular value.

2.5 CONTROLLABILITY, OBSERVABILITY, STABILIZABILITY, AND DETECTABILITY

The LQG/LTR control system design method has a certain requirement of the plant for which the controller is being designed: the plant must be at least stabilizable and detectable. Therefore it is important that the conditions of controllability, observability, and the less restricted conditions of stabilizability and detectability be understood. A description of these concepts will now be presented.

Given the state equation for the system described using Eqs. (2.23) and (2.24), a system is said to be controllable if it is possible to transfer the system from any initial state x_o in state space to any other state x_F using the input in a finite period of time. The system is said to be uncontrollable otherwise. The condition of controllability places no constraint on the input in the system.

The algebraic test for controllability of the LTI system state equation uses the controllability matrix

$$\mathbf{Q} = [\mathbf{B}\ \mathbf{AB}\ \ldots\ \mathbf{A}^{n-1}\mathbf{B}] \quad , \tag{2.45}$$

where n is the number of states. The LTI system is controllable if the rank of Q is equal to n. If the rank of Q is less than n, the system is not controllable. An uncontrollable system indicates that some modes or poles are not affected by the control input. Uncontrollable systems with unstable modes imply that a controller design is not possible to ensure system stability. If the uncontrollable modes of the uncontrollable system are stable, then the system is stabilizable.

Now an observable system will be defined. An LTI system is considered observable at initial time t_0 if there exists a finite time t_1 greater than t_0 such that for any initial state x_0 in state space using knowledge of the input u and output y over the time interval $t_0 < t < t_1$, the state x_0 can be determined. The system is said to be unobservable otherwise.

The algebraic test for observability of the LTI system uses the observability matrix

$$\mathbf{N} = [\mathbf{C}^T\ \mathbf{A}^T\mathbf{C}^T\ \ldots\ (\mathbf{A}^T)^{n-1}\mathbf{C}^T] \quad . \tag{2.46}$$

The LTI system is observable if the rank of **N** is equal to n, where n is the number of states. If the rank of **N** is less than n, the system is unobservable. An unobservable system indicates that not all system modes contribute to the output of the system. If the unobservable modes (states) are stable, then the system is considered to be detectable.

More details regarding the concepts of controllability and observability are found in Refs. 19 and 20.

CHAPTER 3

EVALUATING MULTIVARIABLE PERFORMANCE AND STABILITY ROBUSTNESS OF A CONTROL SYSTEM USING SINGULAR VALUES

3.1 PERFORMANCE ROBUSTNESS

This chapter will define the requirements to obtain a control system that has good performance and stability robustness. The requirements for the control system design are formulated by placing certain restrictions on the singular values of the return ratio, return difference, and inverse return difference of the control system. The block diagram in Fig. 1 shows the controller $[K(s)]$ and plant $[G(s)]$ with input $[d_i(s)]$ and output $[d_0(s)]$ disturbances and sensor noise $[n(s)]$.

Using Fig. 1, a frequency-domain transfer function representation for the plant output is first obtained. These transfer function representations used in conjunction with concepts of singular values allow the formulation of requirements in the frequency domain to obtain a control system with good performance and stability robustness.

In this design, performance robustness is of concern at the output of the plant. Therefore it is required that the plant output transfer function be derived in order to analyze and assist in obtaining a control system design to meet certain performance robustness requirements. Now using Fig. 1, the plant output transfer function is derived and performance robustness requirements established. From Fig. 1 it can be shown that

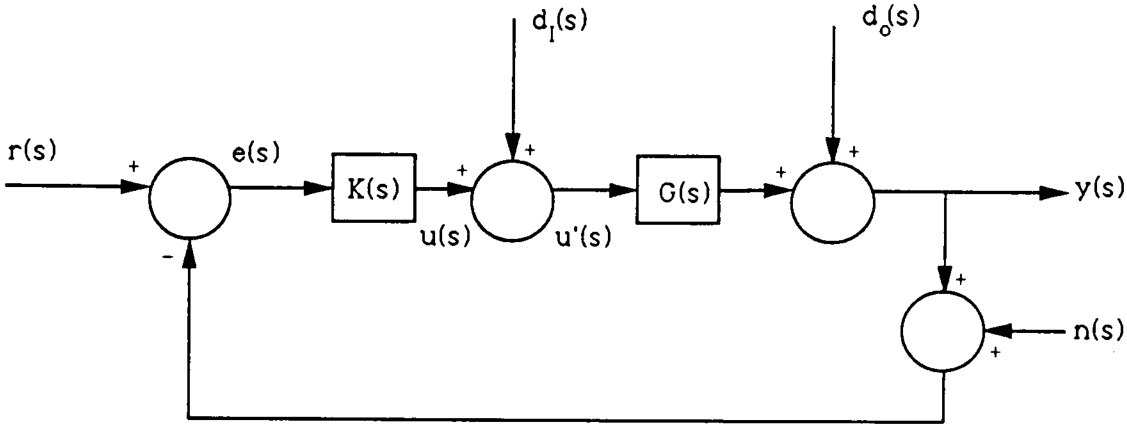

Fig. 1. Model-based unity feedback MIMO control system.

$$y(s) = d_0(s) + G(s)u'(s) \quad , \tag{3.1}$$

$$e(s) = r(s) - y(s) - n(s) \quad , \tag{3.2}$$

and

$$u'(s) = d_I(s) + u(s) = d_I(s) + K(s)e(s) \quad . \tag{3.3}$$

Thus, using Eqs. (3.2) and (3.3), it can be shown that Eq. (3.1) becomes

$$y(s) = [G(s)K(s)][r(s) - y(s) - n(s)] + d_0(s) + G(s)d_I(s)$$

$$y(s) = G(s)K(s)r(s) - G(s)K(s)y(s) - G(s)K(s)n(s) + d_0(s) + G(s)d_I(s) \quad ; \tag{3.4}$$

therefore,

$$\begin{aligned} y(s) &= [I + G(s)K(s)]^{-1}[G(s)K(s)r(s) - G(s)K(s)n(s) + d_0(s) + G(s)d_I(s)] \\ &= [I + G(s)K(s)]^{-1}\{G(s)K(s)[r(s) - n(s)]\} \\ &+ [I + G(s)K(s)]^{-1}[d_0(s) + G(s)d_I(s)] \\ &= y_r(s) + y_{dI}(s) + y_{d0}(s) - y_n(s) \quad , \end{aligned} \tag{3.5}$$

where $y_r(s)$, $y_{d_I}(s)$, $y_{d_0}(s)$ and $y_n(s)$ are, respectively, the contributions to the plant output due to the reference input, input disturbance, output disturbance, and noise input to the system. Now the requirements for good command following, disturbance rejection, and insensitivity to sensor noise will be defined using singular values to characterize the magnitude of MIMO transfer functions. These requirements are also applicable to SISO systems [21].

3.1.1 Command Following

The conditions required to obtain a MIMO control system design with good command following will be described. Good command following of the reference input $r(s)$ by the plant output $y(s)$ implies that

$$y(s) \approx r(s) \;\; \forall s \in s_R \quad , \tag{3.6}$$

where $s = j\omega$ and $s_R = j\omega_R$ and ω_R is the frequency range of the input $r(s)$. Letting $d_0(s) = d_I(s) = n(s) = 0$ in Eq. (3.5) results in

$$y_r(j\omega) = [I + G(j\omega)K(j\omega)^{-1}]G(j\omega)K(j\omega)r(j\omega) \quad ; \;\; \forall \omega \in \omega_R$$

$$y_r(j\omega) = \{G(j\omega)K(j\omega)[I + [G(j\omega)K(j\omega)]^{-1}\}^{-1}G(j\omega)K(j\omega)r(j\omega) \quad ; \quad \forall \omega \in \omega_R$$

$$y_r(j\omega) = \{I + [G(j\omega)K(j\omega)]^{-1}\}[G(j\omega)K(j\omega)]^{-1}G(j\omega)K(j\omega)r(j\omega) \quad ; \quad \forall \omega \in \omega_R$$

$$y_r(j\omega) = \{I + [G(j\omega)K(j\omega)]^{-1}\}^{-1}r(j\omega) \qquad \forall \omega \in \omega_R \; . \tag{3.7}$$

Therefore, to obtain good command following the system inverse return difference $I + [G(j\omega)K(j\omega)]^{-1}$ must have the property such that

$$I + [G(j\omega)K(j\omega)]^{-1} \approx I \quad \forall \omega \in \omega_R \quad , \tag{3.8}$$

which implies that

$$\bar{\sigma}\{I + [G(j\omega)K(j\omega)]^{-1}\} \approx 1 \quad \forall \omega \in \omega_R \tag{3.9}$$

and

$$\bar{\sigma}\{I + [G(j\omega)K(j\omega)]^{-1}\} \leq \bar{\sigma}(I) + \bar{\sigma}\{[G(j\omega)K(j\omega)]^{-1}\} \approx 1 \quad \forall\omega\in\omega_R \ . \tag{3.10}$$

Then

$$1 + \bar{\sigma}\{[G(j\omega)K(j\omega)]^{-1}\} \approx 1 \quad \forall\omega\in\omega_R \ , \tag{3.11}$$

which implies that

$$\bar{\sigma}\{[G(j\omega)K(j\omega)]^{-1}\} << 1 \quad \forall\omega\in\omega_R \ . \tag{3.12}$$

Then using Eq. (2.40) it follows that

$$\bar{\sigma}\{[G(j\omega)K(j\omega)]^{-1}\} = \frac{1}{\underline{\sigma}\{[(G(j\omega)K(j\omega))^{-1}]^{-1}\}} << 1 \quad \forall\omega\in\omega_R \tag{3.13}$$

$$\frac{1}{\underline{\sigma}[G(j\omega)K(j\omega)]} << 1 \quad \forall\omega\in\omega_R \tag{3.14}$$

$$1 << \underline{\sigma}[G(j\omega)K(j\omega)]$$

or

$$\underline{\sigma}[G(j\omega)K(j\omega)] >> 1 \qquad \forall\omega\in\omega_R \ .$$

Thus the magnitude of the return ratio $G(j\omega)K(j\omega)$ must be large over the frequency range of the input to obtain good command following of the control system.

3.1.2 Disturbance Rejection

To minimize the effect of the output disturbance, $y_{d0}(s)$, on the output signal y(s), Eq. (3.5) will be examined when n(s) = r(s) = $d_1(s)$ = 0, which results in

$$y_{d0}(s) = [I + G(s)K(s)]^{-1}d_0(s) \ . \tag{3.15}$$

Rejection of this output disturbance at the plant output requires that the magnitude of the return difference $I + G(s)K(s)$ meet the following condition

$$\underline{\sigma}[I + G(j\omega)K(j\omega)] >> 1 \qquad \forall\omega\in\omega_{d0} \ . \tag{3.16}$$

The requirement of Eq. (3.16) is established to minimize the effect of $y_{d_0}(s)$ on the plant output. Further examination of Eq. (3.16) shows the following using Eq. (2.44)

$$\underline{\sigma}[G(j\omega)K(j\omega)] - 1 \leq \underline{\sigma}[I + G(j\omega)K(j\omega)] \leq \underline{\sigma}[G(j\omega)K(j\omega)] + 1 \quad \forall\omega\in\omega_{d_0} \quad , \tag{3.17}$$

which implies from Eq. (3.16) that it is required that

$$\underline{\sigma}[G(j\omega)K(j\omega)] + 1 >> 1 \qquad \forall\omega\in\omega_{d_0} \, . \tag{3.18}$$

The restriction of Eq. (3.18) also restricts the return ratio such that

$$\underline{\sigma}[G(j\omega)K(j\omega)] >> 1 \quad \forall\omega\in\omega_{d_0} \quad . \tag{3.19}$$

Thus to reject output disturbances, the magnitude of the return ratio must be large.

Now letting r(s) = n(s) = $d_0(s)$ = 0 in Eq. (3.5), the effect of input disturbance on the plant output is examined. This effect is seen to be

$$y_{d_I}(j\omega) = [I + G(j\omega)K(j\omega)]^{-1}G(j\omega)d_I(j\omega) \quad \forall\omega\in\omega_{d_I} \quad , \tag{3.20}$$

where ω_{d_I} is the frequency range of the input disturbance $d_I(s)$. To minimize the effect of $y_{d_I}(j\omega)$ on the plant output requires that the magnitude of the return difference be large (in general, the larger the better). This requirement implies that

$$\underline{\sigma}[I + G(j\omega)K(j\omega)] >> 1 \quad \forall\omega\in\omega_{d_I} \, . \tag{3.21}$$

Following similarly for Eq. (3.16), the return ratio must meet the condition of

$$\underline{\sigma}[G(j\omega)K(j\omega)] \;\; >> 1 \quad \forall\omega\in\omega_{d_I} \tag{3.22}$$

to reject the input disturbance. It should be noted that Eq. (3.22) gives only general conditions for rejection; therefore, how much greater than 1 the return ratio magnitude has to be is determined by the control engineer. This decision probably will be based on prior experience and knowledge of the magnitude of the input disturbance.

3.1.3 Noise Rejection

The requirements to minimize the effects of sensor noise on the plant output will be determined. First letting $r(s) = d_I(s) = d_0(s) = 0$ in Eq. (3.5) results in

$$\begin{aligned} y_n(s) &= [I + G(s)K(s)]^{-1}G(s)K(s)n(s) \qquad \forall s \in s_n \\ &= \{I + [G(s)K(s)]^{-1}\}^{-1}n(s) \quad \forall s \in s_n \end{aligned} \tag{3.23}$$

where $s_n = j\omega_n$ and ω_n is the frequency range of the sensor noise. Thus to minimize the effects of sensor noise on the plant output it is desired to have the magnitude of $y_n(s)$ small over the frequency range of the noise. This indicates that the magnitude of $\{I + [G(s)K(s)]^{-1}\}^{-1}$ is small, which implies that

$$\bar{\sigma}[\{I + [G(j\omega)K(j\omega)]^{-1}\}^{-1}] << 1 \quad \forall \omega \in \omega_n \quad , \tag{3.24}$$

thus using Eq. (2.40), Eq. (3.24) becomes

$$\frac{1}{\underline{\sigma}\{I + [G(j\omega)K(j\omega)]^{-1}\}} << 1 \quad \forall \omega \in \omega_n \tag{3.25}$$

or

$$\underline{\sigma}\{I + [G(j\omega)K(j\omega)]^{-1}\} >> 1 \qquad \forall \omega \in \omega_n \quad . \tag{3.26}$$

Using Eq. (2.44) it can be stated that

$$\underline{\sigma}\{[G(j\omega)K(j\omega)]^{-1}\} - 1 \leq \underline{\sigma}\{I + [G(j\omega)K(j\omega)]^{-1}\} \leq \underline{\sigma}\ \{[G(j\omega)K(j\omega)]^{-1}\} + 1 \quad . \tag{3.27}$$

Therefore the more strict condition of

$$\underline{\sigma}[G(j\omega)K(j\omega)]^{-1} + 1 >> 1 \quad \forall \omega \in \omega_n \tag{3.28}$$

or

$$\underline{\sigma}\{[G(j\omega)K(j\omega)]^{-1}\} >> 1 \quad \forall \omega \in \omega_n \quad , \tag{3.29}$$

which implies that

$$\underline{\sigma}\{[G(j\omega)K(j\omega)]^{-1}\} = \frac{1}{\bar{\sigma}[G(j\omega)K(j\omega)]} >> 1 \quad \forall \omega \in \omega_n \tag{3.30}$$

or

$$\bar{\sigma}[G(j\omega)K(j\omega)] << 1 \quad \forall\omega\in\omega_n \tag{3.31}$$

is required to minimize the effect of noise on the plant output. Thus again the control system return ratio is used to establish another bound in the design process to ensure good performance robustness at the plant output.

It is apparent that any overlapping of any of the frequency ranges ω_R, ω_{d_I}, ω_{d_0}, or ω_n will require system design specification trade-offs to be made. This will definitely occur when overlapping of the lower frequency ranges of ω_R and/or ω_{d_I} and ω_{d_0} with the higher frequency range ω_n occurs.

3.2 STABILITY ROBUSTNESS

All linear control system design methods are based on a linear model of the plant. Because this design model only approximates the actual plant, an error exists between the design model and the actual plant. This error can be evaluated as absolute or relative. The method of evaluation of this error (model uncertainty) depends on the nature of the differences between the actual design model and the actual plant. The evaluation of an absolute error defines an additive model uncertainty, whereas the evaluation of a relative error defines a multiplicative model uncertainty. The additive and multiplicative model uncertainties can be further classified as either structured or unstructured model uncertainties [18,22].

A structured model uncertainty is usually a low-frequency phenomenon characterized by variations in the parameters of the linear time invariant plant design model. These parameter variations are caused by changes in the plant operating conditions, wear due to aging, and environmental conditions. A structured uncertainty also indicates that the gain and phase information concerning the uncertainty is known. Additive model uncertainties are generally considered structured uncertainties.

An unstructured uncertainty is typically a high-frequency phenomenon in which the only information known about the uncertainty is its magnitude. Unstructured uncertainties usually have the characteristic of becoming significant at high frequencies. Multiplicative uncertainties are characterized as unstructured. Unstructured uncertainties are usually caused by the truncation of high-frequency plant dynamics or modes due to the linearization process, and the neglect of plant dynamics such as actuators and sensors. Some plant dynamics that characterize unstructured uncertainty are flexible body dynamics, electrical and mechanical resonances, and transport delays. Most linear control system design methods do neglect these high-frequency plant dynamics. The result is that if a high-frequency bandwidth controller is implemented, the high-frequency modes could be excited, resulting in an unstable control system [23].

Model uncertainty clearly is seen to impose limitations on the achievable performance of a feedback control system design. Thus this section will focus on the limitations imposed by uncertainty, not on the difficult problem of exact representation of the system uncertainty.

3.2.1 Multiplicative Uncertainty

The multiplicative uncertainty (perturbation) can be represented at either the input or output of the plant, and is called respectively the input multiplicative uncertainty or the output multiplicative uncertainty. The model uncertainty due to actuator and sensor dynamics is modeled respectively as an input or output multiplicative perturbation. A reduced-order model of an already linearized model results in a multiplicative model uncertainty. Time delay at the input or output of a plant yields, respectively, input and output multiplicative uncertainties in the plant. Even though other multiplicative model uncertainties exist among various types of control system design problems, the model uncertainties mentioned above appear to be a common consideration in most control problems.

Because in this control problem the concern is the robustness and stability of the plant output, the derivation of the output multiplicative model uncertainty and the conditions for stability will be examined in this section. A block diagram of a control system with a output multiplicative perturbation is shown in Fig. 2. The actual design model or nominal transfer function, and the actual design model with model uncertainty included (perturbed transfer function) are defined respectively as $G(s)$ and $G'(s)$. The plant multiplicative model uncertainty is defined using the concept of relative error as follows

$$\Delta G(s) = [G'(s) - G(s)]\, G^{-1}(s) \tag{3.32}$$

or

$$\Delta G(s) = G^{-1}(s)[G'(s) - G(s)] \tag{3.33}$$

where Eqs. (3.32) and (3.33) are respectively the output and input multiplicative model uncertainties. Considering this problem's interest in the output uncertainty, the perturbed transfer function is defined as

$$G'(s) = L(s)G(s) \tag{3.34}$$

where $L(s)$ represents dynamics not included in the nominal plant $G(s)$. Substituting Eq. (3.34) into Eq. (3.32) results in the output model uncertainty of

$$\Delta G(s) = [L(s) - I] \quad . \tag{3.35}$$

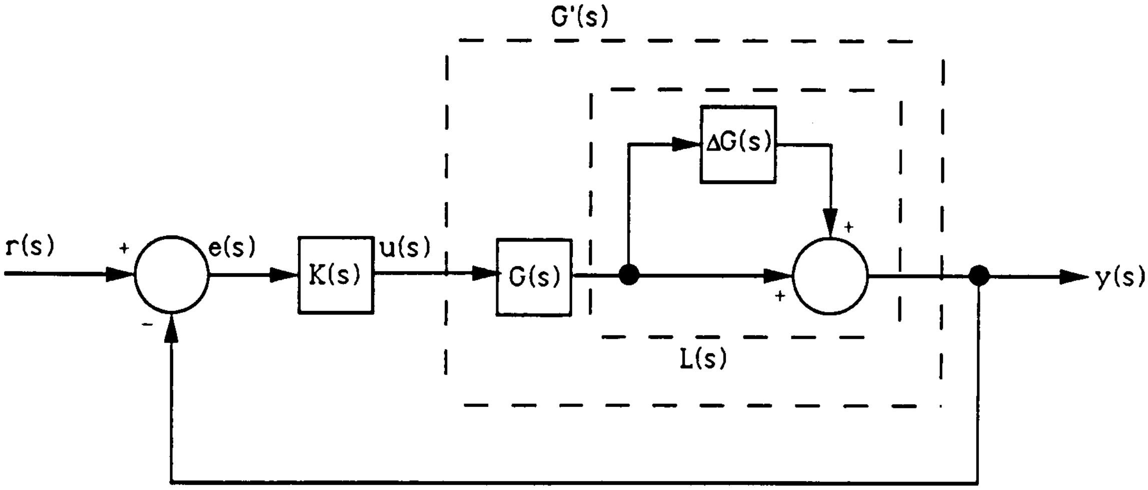

Fig. 2. Control system with output multiplicative perturbation.

The conditions of stability for the control system, considering the limitations due to model uncertainty of the nominal plant or perturbed transfer function represented as

$$G'(j\omega) = [\mathrm{I} + \Delta G(j\omega)]G(j\omega) \quad , \tag{3.36}$$

require that

$$\underline{\sigma}\{\mathrm{I} + [G(j\omega)K(j\omega)]^{-1}\} > \ell_m(\omega) \quad \forall\omega>0 \tag{3.37}$$

where

$$\bar{\sigma}[\Delta G(j\omega)] < \ell_m(\omega) \quad . \quad \forall\omega>0 \tag{3.38}$$

and $\ell_m(.)$ is a positive scalar function confining $G'(j\omega)$ to a neighborhood of $G(j\omega)$ with magnitude $\ell_m(\omega)$.

3.2.2 Additive Uncertainty

The block diagram of a control system with a plant additive model uncertainty is shown in Fig. 3. The representation of the additive model uncertainty using an absolute error criterion is defined as

$$\Delta G(s) = G'(s) - G(s) \tag{3.39}$$

where in this case

$$G'(s) = [\mathbf{C} + \Delta\mathbf{C}]\{s\mathbf{I} - [\mathbf{A} + \Delta\mathbf{A}]\}^{-1}[\mathbf{B} + \Delta\mathbf{B}] \tag{3.40}$$

and

$$G(s) = \mathbf{C}[s\mathbf{I} - \mathbf{A}]^{-1}\mathbf{B} \tag{3.41}$$

where **A**, **B**, and **C** are the nominal system matrices and $\Delta\mathbf{A}$, $\Delta\mathbf{B}$, and $\Delta\mathbf{C}$ are the perturbation matrices that indicate the respective deviations from the nominal system matrices. The perturbation from the nominal system matrices is due to varying the nominal operating conditions. For instance, changing the power output of a reactor from a nominal operating condition of 10% power to a new operating condition of 100% power will cause a perturbation from the nominal system matrices. This perturbation could result in a controller designed to operate at 10% power becoming unstable when suddenly required to operate at other power levels.

In this section the criteria for stability of a plant with additive perturbation will be presented and an explicit representation of the perturbation $\Delta G(s)$ in a convenient state space form will be obtained. The representation of $\Delta G(s)$ in state space form simplifies the propagation of $\Delta G(s)$ in the frequency domain over the use of Eq. (3.39). The condition for stability of the additively perturbed control system requires [24] that

$$\bar{\sigma}\{\mathbf{I} + G(j\omega)K(j\omega)]^{-1}\Delta G(j\omega)K(j\omega)\} < 1 \quad , \tag{3.42}$$

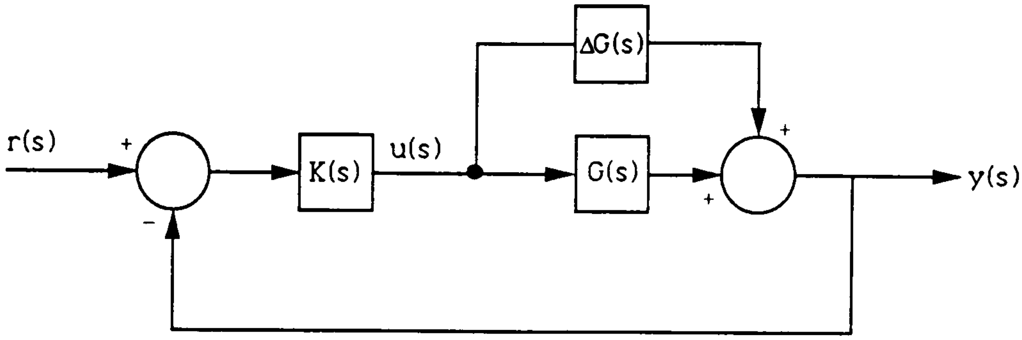

Fig. 3. Control system with additive perturbation.

or more simply

$$\underline{\sigma}[G(j\omega)K(j\omega)] > \bar{\sigma}[\Delta G(j\omega)K(j\omega)] \quad . \tag{3.43}$$

The state space representation of $\Delta G(s)$ is derived as follows: In this derivation the matrix norm of the perturbation matrices $\Delta \mathbf{A}$, $\Delta \mathbf{B}$, and $\Delta \mathbf{C}$ are small so that the first-order approximations of that matrix inverse property

$$[\mathbf{I} - \mathbf{M}]^{-1} \approx [\mathbf{I} + \mathbf{M}] \tag{3.44}$$

can be used in the derivation. Let us define the argument of the resolvent in Eq. (3.40) as

$$\begin{aligned} s\mathbf{I} - [\mathbf{A} + \Delta\mathbf{A}] &= s\mathbf{I} - \mathbf{A} - \Delta\mathbf{A} \\ &= \{\mathbf{I} - \Delta\mathbf{A}[s\mathbf{I} - \mathbf{A}]^{-1}\}[s\mathbf{I} - \mathbf{A}] \quad , \end{aligned} \tag{3.45}$$

and its inverse becomes

$$\begin{aligned} [s\mathbf{I} - (\mathbf{A} + \Delta\mathbf{A})^{-1}] &= \{[\mathbf{I} - \Delta\mathbf{A}(s\mathbf{I} - \mathbf{A})^{-1}][s\mathbf{I} - \mathbf{A}]\}^{-1} \\ &= [s\mathbf{I} - \mathbf{A}]^{-1}[\mathbf{I} - \Delta\mathbf{A}(s\mathbf{I} - \mathbf{A})^{-1}]^{-1} \quad . \end{aligned} \tag{3.46}$$

The perturbed transfer function now becomes

$$G'(s) = [\mathrm{C} + \Delta\mathrm{C}]\{[s\mathrm{I} - \mathrm{A}]^{-1}[\mathrm{I} - \Delta\mathrm{A}(s\mathrm{I} - \mathrm{A})^{-1}]^{-1}\}[\mathrm{B} + \Delta\mathrm{B}]$$

$$= \mathrm{C}[s\mathrm{I} - \mathrm{A}]^{-1}[\mathrm{I} + \Delta\mathrm{A}(s\mathrm{I} - \mathrm{A})^{-1}][\mathrm{B} + \Delta\mathrm{B}]$$

$$+ \Delta\mathrm{C}[s\mathrm{I} - \mathrm{A}]^{-1}[\mathrm{I} + \Delta\mathrm{A}(s\mathrm{I} - \mathrm{A})^{-1}][\mathrm{B} + \Delta\mathrm{B}] \tag{3.47}$$

$$= \mathrm{C}[s\mathrm{I} - \mathrm{A}]^{-1}[\mathrm{I} + \Delta\mathrm{A}(s\mathrm{I} - \mathrm{A})^{-1}]\mathrm{B} + \mathrm{C}[s\mathrm{I} - \mathrm{A}]^{-1}[\mathrm{I} + \Delta\mathrm{A}(s\mathrm{I} - \mathrm{A})^{-1}]\Delta\mathrm{B}$$

$$+ \Delta\mathrm{C}[(s\mathrm{I} - \mathrm{A})^{-1}][\mathrm{I} + \Delta\mathrm{A}(s\mathrm{I} - \mathrm{A})^{-1}]\mathrm{B}$$

$$+ \Delta\mathrm{C}[s\mathrm{I} - \mathrm{A}]^{-1}[\mathrm{I} + \Delta\mathrm{A}(s\mathrm{I} - \mathrm{A})^{-1}]\Delta\mathrm{B} \quad . \tag{3.48}$$

Now eliminating the second-order term of Eq. (3.48) it follows that

$$G'(s) \approx \mathrm{C}(s\mathrm{I} - \mathrm{A})^{-1}\mathrm{B} + \mathrm{C}(s\mathrm{I} - \mathrm{A})^{-1}\Delta\mathrm{A}(s\mathrm{I} - \mathrm{A})^{-1}\mathrm{B} + \mathrm{C}(s\mathrm{I} - \mathrm{A})^{-1}\Delta\mathrm{B}$$

$$+ \Delta\mathrm{C}(s\mathrm{I} - \mathrm{A})^{-1}\mathrm{B} \quad . \tag{3.49}$$

Using Eqs. (3.49) and (3.41) the perturbation transfer function $\Delta G(s)$, Eq. (3.39), is defined as

$$\Delta G(s) = \mathrm{C}(s\mathrm{I} - \mathrm{A})^{-1}\Delta\mathrm{B} + \Delta\mathrm{C}(s\mathrm{I} - \mathrm{A})^{-1}\mathrm{B} + \mathrm{C}(s\mathrm{I} - \mathrm{A})^{-1}\Delta\mathrm{A}(s\mathrm{I} - \mathrm{A})^{-1}\mathrm{B}$$

$$= [\mathrm{C}(s\mathrm{I} - \mathrm{A})^{-1} \quad \Delta\mathrm{C}(s\mathrm{I} - \mathrm{A})^{-1} + \mathrm{C}(s\mathrm{I} - \mathrm{A})^{-1}\Delta\mathrm{A}(s\mathrm{I} - \mathrm{A})^{-1}] \begin{matrix} \Delta\mathrm{B} \\ \mathrm{B} \end{matrix} \tag{3.50}$$

$$\Delta G(s) = [\mathrm{C} \quad \Delta\mathrm{C}] \begin{matrix} (s\mathrm{I} - \mathrm{A})^{-1} & (s\mathrm{I} - \mathrm{A})^{-1}\Delta\mathrm{A}(s\mathrm{I} - \mathrm{A})^{-1} \\ 0 & (s\mathrm{I} - \mathrm{A})^{-1} \end{matrix} \begin{matrix} \Delta\mathrm{B} \\ \mathrm{B} \end{matrix} \tag{3.51}$$

The inner matrix of Eq. (3.51) is the resolvent of the perturbation transfer function $\Delta G(s)$. It is desired to obtain the expression of the resolvent in order to identify the constant matrix used in realizing the resolvent. The resolvent is defined as

$$\Phi(s) = \begin{matrix} (s\mathrm{I} - \mathrm{A})^{-1} & (s\mathrm{I} - \mathrm{A})^{-1}\Delta\mathrm{A}(s\mathrm{I} - \mathrm{A})^{-1} \\ 0 & (s\mathrm{I} - \mathrm{A})^{-1} \end{matrix} \tag{3.52}$$

$$= [s\mathrm{I} - \mathrm{A}]^{-1} \begin{matrix} \mathrm{I} & \Delta\mathrm{A}(s\mathrm{I} - \mathrm{A})^{-1} \\ 0 & \mathrm{I} \end{matrix}$$

$$= \begin{bmatrix} (sI - A)^{-1} & 0 \\ 0 & (sI - A)^{-1} \end{bmatrix} \left\{ \begin{bmatrix} I & 0 \\ 0 & I \end{bmatrix} + \begin{bmatrix} 0 & \Delta A \\ 0 & 0 \end{bmatrix} \begin{bmatrix} (sI - A)^{-1} & 0 \\ 0 & (I - A)^{-1} \end{bmatrix} \right\}$$

$$= \left\{ \underbrace{\begin{bmatrix} sI & 0 \\ 0 & sI \end{bmatrix}}_{sI'} - \underbrace{\begin{bmatrix} A & 0 \\ 0 & A \end{bmatrix}}_{A'} \right\}^{-1} \left\{ \underbrace{\begin{bmatrix} I & 0 \\ 0 & I \end{bmatrix}}_{I'} + \underbrace{\begin{bmatrix} 0 & \Delta A \\ 0 & 0 \end{bmatrix}}_{\Delta A'} \left\{ \begin{bmatrix} sI & 0 \\ 0 & sI \end{bmatrix} - \begin{bmatrix} A & 0 \\ 0 & A \end{bmatrix} \right\}^{-1} \right\} \tag{3.53}$$

$$\Phi(s) = [(sI' - A')^{-1}[I' + \Delta A(sI' - A')^{-1}] \ . \tag{3.54}$$

Using the concepts of Eqs. (3.44) and (3.46), Eq. (3.54) becomes

$$\Phi(s) = \{[I' - \Delta A'(sI' - A')^{-1}](sI' - A')\}^{-1} \tag{3.55}$$

$$= (sI' - A' - \Delta A')^{-1}$$

$$= \left\{ \begin{bmatrix} sI & 0 \\ 0 & sI \end{bmatrix} - \begin{bmatrix} A & \Delta A \\ 0 & A \end{bmatrix} \right\}^{-1} \tag{3.56}$$

The state equation for the transfer function $\Delta G(s)$ is then

$$\dot{x}_{\Delta G} = \begin{bmatrix} A & \Delta A \\ 0 & A \end{bmatrix} x_{\Delta G} + \begin{bmatrix} \Delta B \\ B \end{bmatrix} u_{\Delta G} \tag{3.57}$$

$$y_{\Delta G} = [C \quad \Delta C] x_{\Delta G} \ . \tag{3.58}$$

Table 1 contains a summary of the general design requirements presented in this chapter to obtain a control system with good performance and stability robustness.

Table 1. General System Design Specifications

System requirements	Range
Good command-following	$\underline{\sigma}\left[G(j\omega)K(j\omega)\right] >> 0\ dB \ \ \forall\ \omega \in \omega_R$
Good disturbance rejection	$\underline{\sigma}\left[G(j\omega)K(j\omega)\right] >> 0\ dB \ \ \forall\ \omega \in \omega_d$
Good immunity to noise	$\overline{\sigma}\left[G(j\omega)K(j\omega)\right] << 0\ dB \ \ \forall\ \omega \in \omega_n$
Good system response to high-frequency modeling error*	$\underline{\sigma}\left\{I + \left[G(j\omega)K(j\omega)\right]^{-1}\right\} > \left\|\Delta G(j\omega)\right\| \ \ \forall\ \omega > 0\ rad/s$
Good insensitivity to parameter variations at low frequencies*	$\underline{\sigma}\left[G(j\omega)K(j\omega)\right] > \overline{\sigma}\left[\Delta G(j\omega)K(j\omega)\right]$

*Note: The $\Delta G(j\omega)$ indicated corresponds to the applicable multiplicative or additive model uncertainty.

CHAPTER 4

MULTIVARIABLE STABILITY MARGINS AND MAXIMUM ALLOWABLE TIME DELAY

4.1 MULTIVARIABLE STABILITY MARGINS

Feedback control system design using classical control design techniques has been used to meet performance specifications and account for model uncertainties. These classical control techniques use gain and phase margin to measure the stability of the system. Many multivariable control systems are treated as single-loop systems by decoupling the plant. Once the plant is decoupled a control system is designed for each plant loop. The stability margins are then examined for each loop to ensure that design specifications are met. These stability margins are very optimistic and do not take into consideration the simultaneous variation of gain and phase in all paths, which is a practical consideration.

This section will present a method of evaluating the multivariable stability margins that takes into consideration simultaneous gain and phase variations in several paths [17]. This method overcomes the shortcomings of examining the gain and phase in a single loop while the gain and phase in the other loops are held constant at their nominal values. Using the minimum singular value of the multivariable feedback system return difference, criteria have been developed to compute the multivariable gain and phase margins. The use of the return difference to obtain these margins of stability is somewhat analogous to the classical techniques of measuring the distance of the Nyquist plot of a SISO feedback system to the (-1) point.

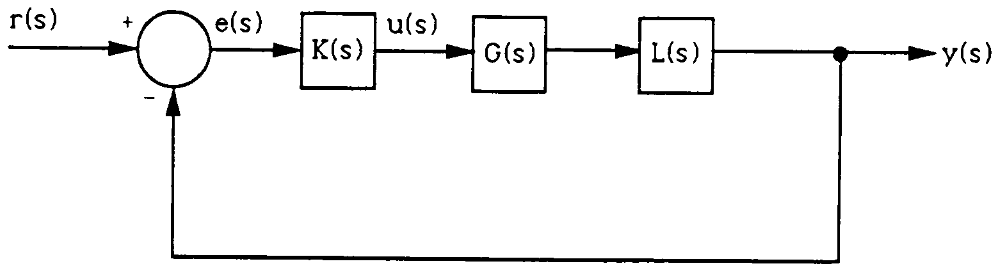

Fig. 4. Unity feedback control system with model uncertainty.

Figure 4 is the block diagram of the unity feedback control system that will be used in stating the conditions to compute the multivariable stability margins (MSMs). The conditions for computing the MSMs will be presented for direct application to the control system design problem in this work.

The transfer function matrices $G(s)$, $K(s)$, and $L(s)$ represent the nominal plant design model, the controller, and the neglected plant dynamics respectively. When $L(s) = I$ the nominal unperturbed loop transfer function is defined as $G(s)K(s)$. The controller $K(s)$ is assumed to be designed using the LQG/LTR procedure. The perturbed loop transfer function is defined as $L(s)G(s)K(s)$ where $L(s) \neq 0$. The perturbed and unperturbed transfer function state space representations are required to have no direct feedthrough from input to output. Also, it is required that both the perturbed and unperturbed transfer function matrices be closed-loop stable.

The minimum singular value of the return difference is very important in characterizing the multivariable gain, phase, and crossover margins. The following conditions and quantities must be met and defined to assist in the characterization:

$$\bar{\sigma}[L^{-1}(j\omega) - I] < \underline{\sigma}[I + G(j\omega)K(j\omega)] \geq 1 \quad , \quad \forall\omega>0 \tag{4.1}$$

$$w(j\omega) = \underline{\sigma}[I + G(j\omega)K(j\omega)] \quad , \quad \forall\omega>0 \tag{4.2}$$

and

$$\alpha_0 = \min_{\omega} w(j\omega) \tag{4.3}$$

where $\alpha_0 \leq 1$. The control weighting matrix **R** is assumed to be large.

Assuming the above conditions hold and

$$\underline{\sigma}[I + G(j\omega)K(j\omega)] \geq \alpha_0 \quad \forall\omega>0 \quad , \tag{4.4}$$

then if $L(j\omega)$ is diagonal such that $L(j\omega) = \text{dia}[\alpha_1, \alpha_2, ..., \alpha_m]$ where α_i is a constant, there is a guaranteed gain margin (GM) defined as

$$GM = \frac{1}{1 \pm \alpha_0} \tag{4.5}$$

that assures stability of the closed-loop perturbed system if the elements of $L(j\omega)$ vary simultaneously as follows:

$$\frac{1}{1 + \alpha_0} < \alpha_i < \frac{1}{1 - \alpha_0} \quad . \tag{4.6}$$

Assuming the same condition for obtaining Eq. (4.5), there is a guaranteed phase margin (PM) of

$$PM = \pm \cos^{-1}\left[1 - \frac{\alpha_0^2}{2}\right] \quad , \tag{4.7}$$

which assures stability of the closed-loop perturbed system if $L(j\omega) = \text{dia}[e^{j\phi_1}, e^{j\phi_2}, ..., e^{j\phi_m}]$ where ϕ_i are constant angles that vary simultaneously as follows:

$$-\cos^{-1}\left[1-\frac{\alpha_0^2}{2}\right] < \phi_i < \cos^{-1}\left[1-\frac{\alpha_0^2}{2}\right] \quad . \tag{4.8}$$

In the case of simultaneous variations for the gains or phase angles, it is assumed that the phase angles and gains are held at their respective nominal values.

The perturbed closed-loop system of Fig. 4, with the previous condition for Eqs. (4.5) and (4.8) holding, can tolerate a crossfeed perturbation of the form

$$L(s) = \begin{bmatrix} I & 0 \\ X(s) & I \end{bmatrix} \tag{4.9}$$

or

$$L(s) = \begin{bmatrix} I & X(s) \\ 0 & I \end{bmatrix} \tag{4.10}$$

with

$$\bar{\sigma}[X(s)] < \alpha_0 \quad . \tag{4.11}$$

The multivariable LQR and the Kalman filter offer very desirable stability margins at their respective input and output. The LQR control system design stability margins are given as follows:

$$GM_{LQR} = 1/2 \quad , \quad \infty \tag{4.12}$$

and

$$PM_{LQR} = \pm\ 60° \tag{4.13}$$

such that

$$1/2 < \alpha_i < \infty \tag{4.14}$$

and

$$-60° < \phi_i < +\ 60° \quad . \tag{4.15}$$

The above results require that the control weighting matrix **R** be diagonal and the state weighting matrix **Q** be positive definite (**Q** > 0), which satisfies the LQR optimal control problem (Appendix A). The nominal LQR control system will tolerate crossfeed perturbation of the form of Eqs. (4.9) and (4.10) and have the guaranteed margins, provided $\mathbf{R} = \rho \mathrm{I}$ where ρ is some positive scalar.

Even though the LQR control system design has nice stability margins, it is really not of practical use. The impracticality is the requirement that all states of the system must be measured, which incurs considerable cost in obtaining sensors. Another limitation of the LQR control system is that it assumes that all states are accessible for measurements, when in reality this is not the case.

To eliminate this problem, the use of the Kalman filter is required to provide state estimates in the control system. The multivariable stability margins of the Kalman filter are the same as the LQR because of the duality property that exists between them. Inclusion of the Kalman filter in the controller structure naturally leads to the formulation of the LQG control system [Appendix B]. This controller has been shown not to have inherently good robustness properties at the plant input or output. However, these good robustness properties are recoverable at either the plant input or output (Appendices B, C, and D) by using the LQG/LTR design technique.

An alternate test of robustness using gain and phase margin criteria can be established using the inverse return difference. This alternate test [25] again leads to analogous conclusions of classical SISO control system design regarding gain and phase margins. A summary of the requirements to use this alternate test are as follows [26]: The matrix transfer function $G(s)K(s)$ is required to be rational and proper and have a closed-loop stable system. The perturbed transfer function $G'(s) = L(s)G(s)$ is closed-loop stable if

(a) $G(s)K(s)$ and $G'(s)K(s)$ have the same number of unstable poles, and

(b) $\bar{\sigma}[L(j\omega) - I] < \underline{\sigma}\{I + [G(j\omega)K(j\omega)]^{-1}\} \quad \forall\omega>0$. (4.16)

It is also assumed that

$$\underline{\sigma}[I + G(j\omega)K(j\omega)] \geq 1 \tag{4.17}$$

to ensure that at least the Kalman filter stability margins at the plant output are achievable. Now let us define

$$\beta_0 = \min_{\omega} (\underline{\sigma}\{I + [G(j\omega)K(j\omega)]^{-1}\}) \quad . \tag{4.18}$$

Thus the guaranteed gain margin (GM) is defined as

$$\mathrm{GM} = 1 - \beta_0 \quad , \quad 1 + \beta_0 \tag{4.19}$$

and the phase margin (PM) is defined as

$$\mathrm{PM} = \pm\sin^{-1}[\frac{\beta_0}{2}] \quad \text{if } \beta_0 < 2 \quad , \tag{4.20}$$

$$= \pm 180^\circ \quad \text{otherwise.}$$

Therefore, closed-loop stability is assured if $L(j\omega) = \mathrm{dia}[\beta_1, \beta_2, ..., \beta_m]$ where α_i are constant gains that vary simultaneously as follows:

$$1 - \beta_0 < \beta_i < 1 + \beta_0 \quad . \tag{4.21}$$

Closed-loop stability is assured if $L(j\omega) = \mathrm{dia}[e^{j\varphi_1}, e^{j\varphi_2}, ..., e^{j\varphi_m}]$ where φ_i are constant angles that vary simultaneously as follows:

$$-2\sin^{-1}\frac{\beta_0}{2} < \varphi_i < 2\sin^{-1}\frac{\beta_0}{2} \quad \text{if } \beta_0 < 2 \quad . \tag{4.22}$$

Stability margins of the LQR and the Kalman filter at both the input and output of the plant can be ensured if both

$$\underline{\sigma}[I + G(j\omega)K(j\omega)] \geq 1 \quad \forall\omega>0 \tag{4.23}$$

and

$$\underline{\sigma}[I + K(j\omega)G(j\omega)] \geq 1 \quad \forall\omega>0 \tag{4.24}$$

are satisfied [17] respectively. Table 2 summarizes the relations to compute the phase and gain margins for multiplicative perturbations.

Also, an important aspect of the stability of MIMO control systems is the ability to maintain stability in the face of actuator/sensor failures [18]. The ability to design a control system with failure integrity is possible using the singular-value analysis and design concepts of the LQG/LTR technique. The design requirement to obtain a system capable of remaining stable in the presence of actuator failures is

$$\underline{\sigma}\{I + [K(j\omega)G(j\omega)]^{-1}\} > 1 \quad \forall\omega>0 \quad . \tag{4.25}$$

4.2 MAXIMUM ALLOWABLE TIME DELAY

Knowledge of the allowable tolerances of gain and phase variations for multiplicative perturbations is seen to be of great use in determining closed-loop system stability. In the SISO case the phase margin and gain crossover frequency information can be used together to determine control system tolerance to a particular system multiplicative perturbation—time delay. The maximum allowable time delay (MATD) a SISO control system can tolerate before instability occurs is defined as

$$\tau \leq \frac{\phi_m \left(\frac{\pi}{180^\circ}\right)}{\omega_c} \tag{4.26}$$

where

τ is in seconds, ϕ_m is the phase margin, and ω_c is the gain crossover frequency.

Table 2. Computation of Phase and Gain Margins for Output Multiplicative Perturbation

Computation of Gain and Phase Tolerance Using	
$\alpha_o = \min_{\omega} \left\{ \underline{\sigma} \left[I + G(j\omega) K(j\omega) \right] \right\}$	$\beta_o = \min_{\omega} \left(\underline{\sigma} \left\{ I + \left[G(j\omega) K(j\omega) \right]^{-1} \right\} \right)$
$GM = \frac{1}{1+\alpha_o}, \frac{1}{1-\alpha_o} \quad if\ 0 < \alpha_o < 1$ $= \frac{1}{1+\alpha_o}, \infty \quad 1 \le \alpha_o$ $PM = -2\sin^{-1}\left(\frac{\alpha_o}{2}\right), 2\sin^{-1}\left(\frac{\alpha_o}{2}\right) \quad if\ \alpha_o < 2$ $= -180^\circ, +180^\circ \quad 2 \le \alpha_o$	$GM = 1 - \beta_o\ ,\ 1 + \beta_o$ $PM = -2\sin^{-1}\left(\frac{\beta_o}{2}\right), 2\sin^{-1}\left(\frac{\beta_o}{2}\right) \quad if\ \beta_o < 2$ $= \pm 180^\circ \quad otherwise$

Note: The gain and phase margins are not restricted to a single frequency as implied above. The gain and phase margins for MIMO systems, unlike SISO systems, can be computed for various frequencies.

The MATD that a highly coupled MIMO control system can tolerate before it destabilizes is not as easily answered as it was for the SISO system. However, using a modern technique based on singular values applicable to either a SISO or MIMO system, the maximum allowable time delay is obtainable. This modern method of computing maximum allowable time delay to maintain closed-loop stability is presented in Ref. 27. Assuming that the nominal closed loop control system is stable, this method can be applied to a SISO or a MIMO control system. The general block diagram of the control system with time delay is shown in Fig. 5.

Computing the MATD for a SISO control system requires

$$\tau < \inf\{(2/\omega)\sin^{-1} \frac{1}{2M(\omega)} \ : \omega \in \Omega\} \quad , \tag{4.27}$$

where

$$M(\omega) = \left| \frac{G(j\omega)K(j\omega)}{1 + G(j\omega)K(j\omega)} \right| \quad , \tag{4.28}$$

ω is frequency in radians per second, and Ω is the frequency range such that

$$M(\omega) \geq 0.5 \quad . \tag{4.29}$$

The multivariate extension of this method requires that

$$\tau = \min\,[\tau_i : i = 1, 2, ..., n] \tag{4.30}$$

where

$$\tau_i < \inf\,\{(2/\omega)\sin^{-1}[\frac{1}{2\sigma_i(\omega)}] : \omega \in \Omega_i\} \quad , \tag{4.31}$$

σ_i is the *ith* singular value of $G(j\omega)K(j\omega)[I + G(j\omega)K(j\omega)]^{-1}$, and Ω_i is the frequency range such that $\sigma_i \geq 0.5$.

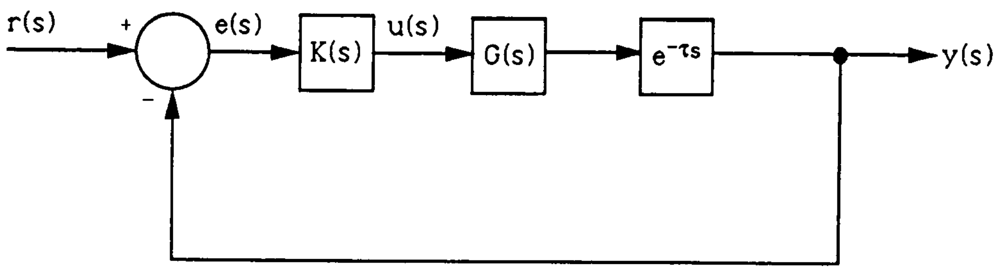

Fig. 5. Unity feedback control system with time delay.

The use of this method with MIMO control systems narrows the gap between analogous classical and modern frequency domain analysis techniques. Time delay in a system is classified as a multiplicative uncertainty (perturbation). Using tools of analysis, the limits of stability due to the time delay can be classified easily in terms of phase andgain tolerances. Using the modern method of computing MATD, the control system ability to tolerate time delay can be easily identified. It appears, however, that classifying the limits of stability due to phase and gain is less useful than identifying the MATD.

CHAPTER 5

EFFECTS OF NONMINIMUM PHASE ZERO ON SISO AND MIMO SYSTEMS

5.1 NONMINIMUM PHASE ZERO LIMITATION ON SINGLE-INPUT/SINGLE-OUTPUT SYSTEMS

Classical control system design methods have extensively analyzed the behavior of minimum phase transfer functions with and without a nonminimum phase zero. Typically Bode's integral theorem has been used to examine the relationship between the gain and phase of a transfer function, specifically the phase $\{\phi(\omega_c) = arg[g(j\omega_c)k(j\omega_c)]\}$ near gain crossover $[\underline{\sigma} = \bar{\sigma} = 1 = g(j\omega_c)k(j\omega_c)]$. The interest in what occurs at gain crossover is because the phase $[\phi(\omega_c)]$ can be computed and used to give a relative idea of the stability of the system. Also, according to Bode's integral theorem [18] ϕ_m will be large if the gain, which is defined as

$$\underline{\sigma}[g(j\omega)k(j\omega)] = \bar{\sigma}[g(j\omega)k(j\omega)] = |g(j\omega)k(j\omega)| \tag{5.1}$$

for the SISO system, attenuates slowly and small if the gain attenuates rapidly. Thus the magnitudes of the return difference $[1 + g(j\omega)k(j\omega)]$ and the inverse return difference $\{1 + [g(j\omega)k(j\omega)]^{-1}\}$ are affected by the size of $\phi(j\omega_c)$. Let us examine the case when $|g(j\omega)k(j\omega)| = 1$ where $\omega = \omega_c$ and $\phi_m = \phi(j\omega_c)$. To illustrate this let us redefine the loop return ratio $g(j\omega)k(j\omega)$ at the gain crossover frequency (ω_c) in terms of the phase margin ϕ_m as follows:

$$g(j\omega_c)k(j\omega_c) = 1\underline{/\phi(\omega_c)}$$

$$= 1\underline{/180°}[1\underline{/180° + \phi(\omega_c)}]$$

$$= -1\underline{/\phi_m} \tag{5.2}$$

$$L(j\omega) = -[\cos(\phi_m) + j\sin(\phi_m)]$$

where $\phi_m = 180° + \phi(\omega_c)$ is the phase margin and L(jω) is the return ratio of the SISO system expressed as a function of phase margin. Considering the stability robustness and performance criteria dictated by the inverse return difference and return difference at $|g(j\omega_c)k(j\omega_c)| = 1$, then

$$|1 + g(j\omega_c)k(j\omega_c)| = |1 + [g(j\omega_c)k(j\omega_c)]^{-1}| = |1 + L(j\omega_c)|$$

$$= |1 - \cos(\phi_m) - j\sin(\phi_m)|$$

$$= \sqrt{[1 - \cos(\phi_m)]^2 + \sin^2\phi_m}$$

$$= \sqrt{[1 - 2\cos(\phi_m) + \cos^2(\phi_m)] + \sin^2\phi_m}$$

$$= \sqrt{2 - 2\cos(\phi_m)}$$

$$= \sqrt{2}\sqrt{1 - \cos(\phi_m)} \tag{5.3}$$

or Eq. (5.3) can be expressed [27] as

$$\sqrt{2}\sqrt{1 - \cos(\phi_m)} = 2\sqrt{\frac{1 - \cos(\phi_m)}{2}}$$

$$= 2\left|\sin\frac{\phi_m}{2}\right| \ . \tag{5.4}$$

Thus it can be seen from Eq. (5.3) that as the phase margin gets small the return difference and the inverse return difference get smaller. The implications of the return difference getting small indicates that output plant disturbance $[d_0(s)]$ is amplified at the crossover frequency (ω_c) and the surrounding region provided the phase margin (ϕ_m) is small. The ability to tolerate model uncertainty near ω_c is reduced significantly due to the small magnitude of the inverse return difference. Thus as the rate of attenuation of the magnitude (dB/decade) increases, the poorer are the performance and stability robustness qualities near the crossover frequency.

The presence of nonminimum phase zeros diminishes any loop properties of the system only near the crossover frequency. Considering that a plant with rhp zeros can be factored as

$$g'(s) = \ell(s)g(s) \tag{5.5}$$

where $g(s)$ is minimum phase, and $\ell(s)$ is an all-pass factor such that

$$\ell(s) = \frac{(s - z_1)(s - z_2) \ldots (s - z_q)}{(s + z_1)(s + z_2) \ldots (s + z_q)} \tag{5.6}$$

where $z_1, z_2, \ldots, z_q$ are rhp zeros and

$$|\ell(s)| = 1 \quad \forall\omega \quad . \tag{5.7}$$

The presence of rhp zeros in Eq. (5.6) contributes a negative phase angle that reduces the phase margin at crossover and thus reduces system stability. The phase at the gain crossover frequency for the plant described by Eq. (5.5) is as follows:

$$\phi_m = \phi_0 + \phi_\ell \tag{5.8}$$

where ϕ_0 is the phase of the minimum phase plant $g(s)$ and ϕ_ℓ is the phase of the all-pass factor $\ell(s)$. The effect of the presence of rhp zeros within the bandwidth of the minimum phase plant [$g(s)$] creates greater difficulty in the control system design. However, if the rhp zeros are significantly beyond the system's bandwidth, then they pose little difficulty in obtaining a control system design. Thus rhp zeros limit the plant's bandwidth (analogously loop gain) in a manner similar to a plant model uncertainty. The all-pass factor $\ell(s)$ therefore results in a model uncertainty defined as

$$\Delta g(s) = |1 - \ell(s)| \quad , \tag{5.9}$$

which limits a minimum phase control system design of the plant $g(s)$ in the following manner

$$|1 - \ell(j\omega)| < |1 + [g(j\omega)]^{-1}| \quad \forall\omega>0 \quad . \tag{5.10}$$

Another important characteristic of a system with rhp zeros (nonminimum phase) is that the initial time response of the system is negative despite the fact that the final steady state value is positive. This behavior exists for both the SISO and MIMO systems that are nonminimum phase. Also, for both SISO and MIMO systems the zeros of the open-loop system are the same as the zeros of the closed-loop system with unity feedback. Therefore, significant increases in the system gain in a nonminimum phase SISO or MIMO system will result in the closed-loop system going unstable due to migration of the root loci from poles in the left hand s-plane to the rhp zeros.

5.2 NONMINIMUM PHASE ZERO LIMITATION ON MULTIPLE INPUT/ MULTIPLE OUTPUT (MIMO) SYSTEMS

Nonminimum phase MIMO systems have the same limitations as SISO systems. The concept of crossover for a MIMO system is, however, different from crossover for SISO systems. In MIMO systems there exists a region in the frequency domain in which the singular values of the system are near or equal to 1, and there is no single frequency at which the crossover frequency is characterized. However, in formulating a control system design using a technique such as LQG/LTR the resulting return ratio (open-loop transfer function) for the system can yield singular values that are all 1 at the same crossover frequency.

Another characteristic of MIMO systems is that Bode's integral theorem is not applicable to singular values. Thus singular values of rational, stable, proper minimum phase MIMO transfer function cannot be used to compute the phase angle of the system near crossover. The singular value cannot be used because it is a function of a complex variable and therefore is not analytic and cannot be used in the contour integration of Bode's integral theorem. Eigenvalues do not have this problem but lack any direct relationship to the quality of performance and stability robustness as described for the singular values in Chapter 3. The singular values and the eigenvalues are related, however, through a bounding relation for a square matrix. Eigenvalues relate to singular values in the following manner:

$$\underline{\sigma}[GK] \leq \lambda[GK] \leq \bar{\sigma}[GK] \quad . \tag{5.11}$$

The gain/phase relation for MIMO systems can be obtained using the eigenvalues of $I + GK$ (return difference) and $I + (GK)^{-1}$ (inverse return difference) in a manner similar to SISO systems. Also, the eigenvalues of the return difference and the inverse return difference offer some idea of the quality of the system's performance and stability robustness because of the relationship to singular values as shown in Eq. (5.11). The eigenvalues of the return difference and inverse return difference are represented as follows

$$\lambda_i[I + G(j\omega)K(j\omega)] = 1 + \lambda_i[G(j\omega)K(j\omega)] \tag{5.12}$$

and

$$\lambda_i\{I + [G(j\omega)K(j\omega)]^{-1}\} = 1 + \frac{1}{\lambda_i[G(j\omega)K(j\omega)]} \quad . \tag{5.13}$$

At the gain crossover frequency ($\omega = \omega_c$) $|\lambda_i[G(j\omega_c)K(j\omega_c)]| = 1$, which implies that

$$|\lambda_i[G(j\omega_c)K(j\omega_c)]| = |\lambda_i\{I + [G(j\omega_c)K(j\omega_c)]^{-1}\}|$$

$$= 2\left|\sin\left(\frac{\pi + \phi_{\lambda_{ic}}}{2}\right)\right|$$

$$= 2\left|\sin\left(\frac{\phi_{m\lambda_i}}{2}\right)\right| \tag{5.14}$$

$$= 2\sqrt{\frac{1 - \cos\phi_{m\lambda_i}}{2}} \quad , \tag{5.15}$$

where $\phi_{m\lambda_i} = \pi + \phi_{\lambda_{ic}}$ is a phase angle, which when small indicates that the system has poor properties. The angle $\phi_{\lambda_{ic}}$ is computable using the integral relation [18]

$$\sum_i \phi_{\lambda_{ic}} = \frac{1}{\pi}\int_{-\infty}^{\infty} \sum_i \frac{\{\ell n\,|\lambda_i[j\omega(\nu)]| - \ell n\,|\lambda_i(j\omega_c)|\}}{\sinh\,(\nu)}\,d\nu \tag{5.16}$$

where $\nu = \ell n(\omega/\omega_c)$. Assuming the singular values are balanced at the crossover frequency, ω_c which implies $\sigma_i = 1$. This further indicates that at ω_c for every i, $\lambda_i = 1$ and $\phi_{\lambda_{ic}}$ are the same. The multivariable return ratio therefore imposes the same limitations as the SISO system in terms of rate of attenuation and system quality at gain crossover.

The multivariable generalizations described above are applicable to minimum phase systems. The presence of rhp zeros in a MIMO system contributes a negative phase angle to the phase angle described in Eq. (5.16). Thus the rhp zeros degrade the MIMO system loop properties in a manner analogous to the SISO system. The MIMO plant transfer function with rhp transmission zeros can be expressed as

$$G'(s) = L(s)G(s) \tag{5.17}$$

where $G(s)$ is the minimum phase plant and $L(s)$ is an all-pass transfer function such that

$$L^T(-j\omega)L(j\omega) = I \quad \forall\omega \quad . \tag{5.18}$$

The rhp zeros can be characterized as model uncertainties at the plant output or plant input respectively. The model uncertainty of interest in this work is the output model uncertainty. Using $L(s)$, the output model uncertainty due to the rhp transmission zeros is defined as

$$\Delta G(s) = [I - L(s)] \quad . \tag{5.19}$$

This model uncertainty of the MIMO system can be used to constrain the design of the control system to select $K(s)$ for the minimum phase plant $G(s)$ such that $G'(s)K(s)$ yields a stable control system design.

CHAPTER 6

LQG/LTR DESIGN PROCEDURE FOR NONMINIMUM PHASE PLANTS

The purpose of this chapter is to describe the procedure for design of a stable control system of a nonminimum phase plant. This design procedure uses the LQG/LTR design technique with additions and modifications to the existing design and analysis procedure. The present LQG/LTR design technique is applicable to minimum phase plants. The resulting controller guarantees good robustness properties at either the plant output or input. These robustness properties, however, are not guaranteed for a nonminimum phase plant. The nonminimum phase property of the plant is assumed to originate from time delay at the plant output.

The procedure to be presented here will provide a quantitative measure of how time delay degrades the stability robustness of the control system. This procedure will also include an analysis of the maximum allowable time delay before instability occurs in the LQG/LTR control system designed for a plant with time delay. The procedure will further establish a clear connection between the frequency domain stability criteria for plants with time delay and will explain how in application the time domain stability results verify the frequency domain stability results.

It will be shown that by modifying the LQG/LTR design method a more intuitive and analytical approach can be taken in designing a stable control system for a nonminimum phase plant.

6.1 SYSTEM UNCERTAINTY FOR A PLANT DUE TO TIME DELAY

The first step in this procedure of control system design requires the nonminimum phase plant to be factored into a nominal plant matrix transfer function and the matrix transfer functions of time delay and the actuator components at the plant output and input respectively. The perturbed plant described in transfer function form is as follows

$$G'(s) = B_z(s)G(s)B_a(s) \tag{6.1}$$

where $G(s)$ is a minimum phase model of the plant, $B_a(s)$ is the input actuator matrix transfer function, and $B_z(s)$ is the matrix transfer function for input time delay. Considering exact representation of time delay $B_z(s)$ consists of $e^{-\tau s}$ on the matrix transfer function diagonal. The time delay matrix $B_z(s)$ diagonal element $e^{-\tau s}$ can be represented as a low-order Padê approximation

$$e^{-\tau s} \approx \frac{1 - s(\tau/2)}{1 + s(\tau/2)} \quad , \tag{6.2}$$

which is an all-pass filter contributing a nonminimum phase zero to the plant open-loop system where τ is the system time delay. This approximation of time delay is considered valid in this control system design because the model is a finite approximation and the errors in approximating $e^{-\tau s}$ become significant only at higher frequencies. Therefore the mathematical difficulty involved in synthesizing a controller for an exact time delay yields no significant benefits when compared to using the approximation in a low-bandwidth process control system. Figure 6 is the perturbed feedwater control system block diagram.

Ignoring the actuator dynamics, the perturbed transfer function is defined as

$$G'(s) = B_z(s)G(s) \quad , \tag{6.3}$$

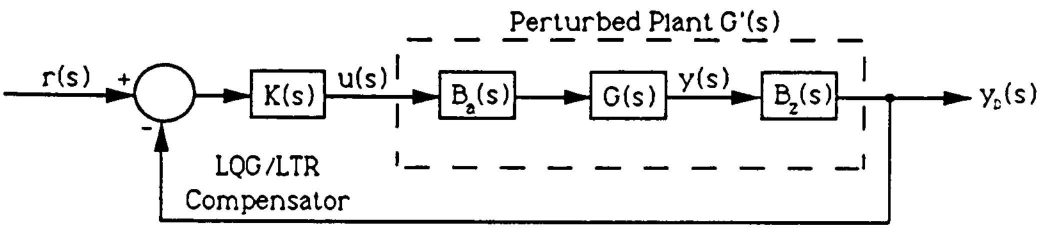

Fig. 6. Perturbed feedwater control system.

assuming the time delay varies uniformly in all channels of the output vector $y(s)$. The actuator dynamics are ignored because the interest here is designing a robust control system at the plant output, and therefore in the design procedure only the output plant perturbations are of interest. The input plant perturbation due to the actuator dynamics can be used after the design is complete to check the effective input stability robustness resulting from the design.

The state equation for the nominal minimum phase transfer function $G(s)$ is defined as

$$\dot{x} = Ax + Bu \tag{6.4}$$

and

$$y = Cx \tag{6.5}$$

where $x \in R^n$, $u \in R^p$, and $y \in R^p$. The letters n and p are respectively the dimensions of the states and the input and output vectors where the number of inputs and outputs are the same dimensions. The system matrices are $A \in R^{n \times n}$, $B \in R^{n \times p}$, and $C \in R^{p \times n}$.

The state equation for $B_z(s)$ using Eq. (6.2) is defined as

$$
\dot{x}_D = \begin{bmatrix} \dot{x}_{D1} \\ \dot{x}_{D2} \\ \vdots \\ \dot{x}_{Dp} \end{bmatrix} = \begin{bmatrix} -\frac{2}{\tau_{11}} & 0 & 0 \ldots & 0 \\ 0 & -\frac{2}{\tau_{22}} & 0 \ldots & 0 \\ 0 & 0 & -\frac{2}{\tau_{33}} & \vdots \\ 0 & 0 & 0 & -\frac{2}{\tau_{PP}} \end{bmatrix} \begin{bmatrix} x_{D1} \\ x_{D2} \\ \vdots \\ x_{DP} \end{bmatrix} + \begin{bmatrix} 1 & 0 & & & \ldots & 0 \\ 0 & 0 & 1 & 0 & \ldots & 0 \\ \vdots & 0 & 0 & 1 & 0\ldots & 0 \\ & & & & & \vdots \\ 0 & 0 & 0 & 0 & 0 & 1 \end{bmatrix} \begin{bmatrix} y_1 \\ y_2 \\ \vdots \\ y_P \end{bmatrix} \tag{6.6}
$$

$$
y_D = \begin{bmatrix} y_{D1} \\ y_{D2} \\ \vdots \\ y_{DP} \end{bmatrix} = \begin{bmatrix} \frac{4}{\tau_{11}} & 0 & 0 & 0 \\ 0 & \frac{4}{\tau_{22}} & 0 & 0 \\ \vdots & \vdots & & \vdots \\ 0 & 0 & 0 & \frac{4}{\tau_{PP}} \end{bmatrix} \begin{bmatrix} x_{D1} \\ x_{D2} \\ \vdots \\ x_{DP} \end{bmatrix} + \begin{bmatrix} -1 & 0 & 0 & 0 \\ 0 & -1 & 0 & 0 \\ & & & \vdots \\ 0 & 0 & 0 & -1 \end{bmatrix} \begin{bmatrix} y_1 \\ y_2 \\ \vdots \\ y_P \end{bmatrix} \tag{6.7}
$$

where x_{Di} is the state associated with realizing the delay for the *ith* output, y_i is the *ith* plant output, y_D is the delayed plant output vector, and y_{Di} is the delayed output of the *ith* plant output where $i = 1,..., p$. A simplified representation of Eqs. (6.6) and (6.7) is as follows

$$\dot{x}_D = \mathbf{A}_D x_D + \mathbf{B}_D y \tag{6.8}$$

and

$$y_D = \mathbf{C}_D x_D + \mathbf{D}_D y \tag{6.9}$$

where $\mathbf{A}_D \in \mathbf{R}^{P \times P}$, $\mathbf{B}_D \in \mathbf{R}^{P \times P}$, $\mathbf{C}_D \in \mathbf{R}^{P \times P}$, and $\mathbf{D}_D \in \mathbf{R}^{P \times P}$ are the corresponding system matrices of Eqs. (6.6) and (6.7).

The state equations (6.4), (6.5), (6.8), and (6.9) thus can be combined to obtain the output transient response of the perturbed plant of the closed-loop control system when used with the equations of the controller as shown in Fig. 6, assuming $B_a(s) = \mathbf{I}$.

The significance of the required factorization of the plant into minimum and nonminimum phase components is that the nonminimum phase component can be used to characterize a model uncertainty $\Delta G_D(s)$. Using this model uncertainty to establish a stability robustness bound at the plant output, a control system design is obtained using the LQG/LTR technique. The nominal minimum phase plant component is used in the control system design. The model uncertainty $\Delta G_D(s)$ due to time delay thus can be used to ensure stability robustness of the minimum phase plant design, thus also ensuring stability robustness of the nonminimum phase perturbed plant.

The model uncertainty due to the time delay component of the perturbed plant is as follows:

$$\Delta G_D(s) = \mathbf{I} - B_z(s) \quad , \tag{6.10}$$

where $B_z(s)$ is as previously defined.

6.2 MODIFIED LQG/LTR COMPENSATOR DESIGN

This section will describe the LQG/LTR compensator designed for the minimum phase plant described in section 6.1. The control system designed will be guaranteed to be stable and will be robust to the extent dictated by the analytical and intuitive method of this modified procedure.

First, it is assumed that if zero steady state error is desired in the control system design, the plant inputs will be augmented to obtain the desired integral action. In some cases the dynamics of the plant may have poles that are nearly zero, which establishes a near integral action in the plant. In such a case the addition of integrals at the plant input causes a much greater than 20-dB/decade roll-off, thus yielding unreasonable plant dynamics characterized by the return ratio singular-value plots. Therefore caution is required in deciding how or whether to augment the plant dynamics. In the following description of the compensator design it is assumed that the nominal plant $G(s)$ has been augmented as required by the control engineers' desires.

Step 1. The first step requires selecting the appropriate transfer function $[G_{FOL}(s)]$ that satisfies the desired performance and stability robustness of the final control system. Therefore, the appropriate scalar $\mu > 0$ and a constant matrix L such that the singular values of

$$G_{FOL}(s) = (1/\sqrt{\mu})[\mathbf{C}(s\mathbf{I} - \mathbf{A})^{-1} L] \tag{6.11}$$

approximately meet the desired control system requirements. The system matrices C and A of the minimum phase component are assumed to have been augmented already to obtain the necessary integral action. The selection of L is made so that at low frequencies ($s = j\omega \rightarrow 0$), high frequencies ($s = j\omega \rightarrow j\infty$), or intermediate frequencies ($s = j\omega \rightarrow j\omega_I$) the singular values of $G_{FOL}(s)$ are approximately the same [28]. After selecting L then μ is adjusted to obtain the desired crossover frequency of $\bar{\sigma}[G_{FOL}(j\omega)]$; therefore μ functions as a gain parameter of the transfer function. It should be noted that it is desired to balance the singular values of $G_{FOL}(s)$ in the region of the crossover frequency in order to obtain similar responses for each loop of the system. Also, typically it is desired to have the return ratio singular values roll off at a rate no greater than −20 dB/decade in the region of gain crossover.

One additional important design criterion that must be met is the requirement to assure stability of the plant in the presence of time delay. Using the model uncertainty representative of time delay at the plant output given in Eq. (6.10), the requirement for stability robustness is

$$\underline{\sigma}\{\mathbf{I} + [G_{FOL}(s)]^{-1}\} > \bar{\sigma}[\Delta G_D(s)] \quad \forall\omega>0 \quad . \tag{6.12}$$

The inequality of Eq. (6.12) thus ensures stability of the nonminimum phase plant while using a minimum phase design technique.

Step 2. In this step the Kalman filter transfer function is defined as

$$G_{KF}(s) = C(s\mathbf{I} - \mathbf{A})^{-1}F \tag{6.13}$$

where F is the Kalman filter gain and C and **A** are as previously defined. The filter gain will now be obtained.

To compute the filter gain F, first the following Kalman filter algebraic Riccati equation (ARE) is solved

$$LL^T - (1/\mu)\Sigma C^T C\Sigma + \mathbf{A}\Sigma + \Sigma\mathbf{A}^T = 0 \tag{6.14}$$

where L and μ are as obtained in step 1 and Σ (the covariance matrix) is the solution to the equation. The filter gain is thus computed to be

$$F = (1/\mu)\Sigma C^T \quad . \tag{6.15}$$

Thus as seen above, L and μ are tunable parameters used to produce the necessary filter gain F to meet the desired system performance and stability robustness constraints. This step completes the LQG/LTR design requirement of designing the target Kalman filter transfer function matrix with the desired properties which will be recovered at the plant output during the loop transfer recovery step. The general block diagram of the LQG/LTR control system is shown in Fig. 7.

Step 3. The transfer function of the LQG/LTR controller is defined as

$$K(s) = K[s\mathbf{I} - (\mathbf{A} - \mathbf{B}K - FC)]F \tag{6.16}$$

where A, B, and C are the system matrices of Eqs. (6.4) and (6.5). The filter gain F is as stated in Eq. (6.15). The regulator gain K will be computed in this step to achieve loop transfer recovery. The selection of K will yield a return ratio at the plant output such that

$$G(s)K(s) \rightarrow G_{KF}(s) \quad . \tag{6.17}$$

The first step in selecting K requires solving the LQR problem, which has the following ARE

$$Q(q) - S\mathrm{B}R_0^{-1}\mathrm{B}^T S + S\mathrm{A} + \mathrm{A}^T S = 0 \tag{6.18}$$

where $R_0 = \mathrm{I}$ is the control weighting matrix and $Q(q) = Q_0 + q^2 CC^T$ is the modified state weighting matrix. The scalar q is a free design parameter. The resulting regulator gain is computed as

$$K = B^T S \quad . \tag{6.19}$$

As q $\rightarrow$ 0 Eq. (6.18) becomes the ARE to the optimal regulator problem. As q $\rightarrow \infty$ the LQG/LTR technique guarantees that since the design model $G(s) = \mathrm{C}(s\mathrm{I} - \mathrm{A})^{-1}\mathrm{B}$ has no nonminimum phase zeros [18], then pointwise in s

$$\lim_{q \rightarrow \infty} G(s)K(s) \rightarrow G_{KF}(s) \tag{6.20}$$

$$\lim_{q \rightarrow \infty} \{\mathrm{C}(s\mathrm{I} - \mathrm{A})^{-1}\mathrm{B}K[s\mathrm{I} - (\mathrm{A} - \mathrm{B}K - F\mathrm{C})]^{-1}F\} \rightarrow \mathrm{C}(s\mathrm{I} - \mathrm{A})^{-1}F \quad . \tag{6.21}$$

The loop transfer recovery step of Eq. (6.20) is excellent even for the problem formulated here, provided the nonminimum phase zero of $B_z(s)$ is beyond the bandwidth of $G(s)$.

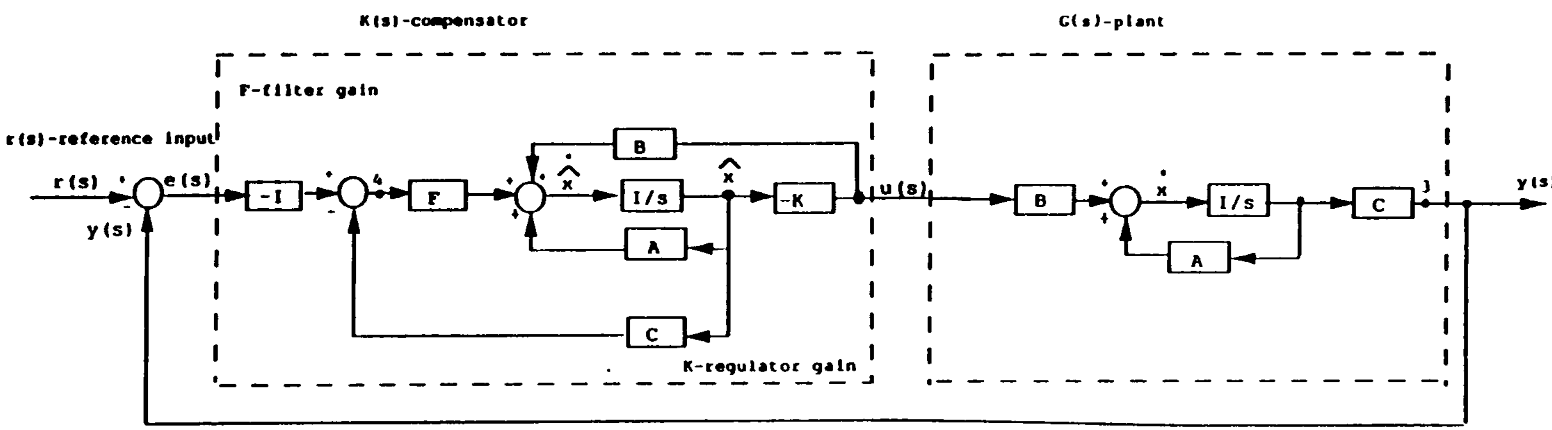

Fig. 7. Block diagram of unity feedback LQG/LTR control system.

Now that the loop transfer recovery step is complete, the singular-value plots of the return ratio, return difference, and inverse return difference of $G(s)K(s)$ are examined to verify that the desirable loop shape has been obtained.

Step 4. In this step the maximum value of time delay that will destabilize the previously designed control system will be obtained using a frequency domain graphical technique and a purely analytical technique.

It is well established [18] that the inequality to examine stability robustness to delay at the output of the control system under consideration is

$$\underline{\sigma}\{I + [G(j\omega)K(j\omega)]^{-1}\} > \bar{\sigma}[\Delta G_D(j\omega)] \quad \forall\omega>0 \tag{6.22}$$

where $\Delta G_D(j\omega)$ was selected initially to reflect the anticipated time delay in the plant. However, by increasing the time delay τ the magnitude of $\Delta G_D(j\omega)$ becomes larger and at some value of τ the inequality of Eq. (6.22) is violated, which indicates that the control system becomes unstable. Plotting $\underline{\sigma}\{I + [G(j\omega)K(j\omega)]^{-1}\}$ and $\bar{\sigma}[\Delta G_D(j\omega)]$ as τ increases the value of τ, which results in a sufficient magnitude of $\bar{\sigma}[\Delta G_D(j\omega)]$ to violate the inequality of Eq. (6.22).

Next the MATD for this control system is computed using an analytical technique described in Chapter 4. The MATD computed using this analytical technique is expected to be conservative in comparison to the MATD obtained using the previously mentioned graphical technique. The conservativeness or lack of conservativeness of the MATD computed using the analytical technique can be verified by plotting $\bar{\sigma}[\Delta G_D(j\omega)]$ using the MATD obtained from both the graphical and analytical method, and $\underline{\sigma}\{I + [G(j\omega)K(j\omega)]^{-1}\}$, then observing which value of time delay comes nearer to violating the inequality for stability robustness.

The validity of which computed time delay [either τ_A(analytical MATD) or τ_G(graphical MATD)] reflects the most realistic MATD to destabilize the control system can be verified by obtaining time responses of the control system as the time delay is increased to destabilize the system. It is expected that whichever time, τ_A or τ_D, comes nearer to violating the inequality of Eq. (6.22) will also be approximately equal to the time delay that destabilizes the system in the time domain. The time domain analysis will also verify which MATD is the most conservative for this control system design.

The analysis of step 4 provides a means to relate the control system stability criteria of singular values in the frequency domain to the stability of the actual control system in the time domain for plants with time delay. Incorporating this type of analysis into the modified LQG/LTR design procedure allows a more practical idea of the time delay stability robustness implications for two methods of computing MATD and how it relates to the actual system. This relation between the frequency and time domain allows the control engineer to capture some of the intuitiveness of the SISO control system design method in a very analytical MIMO control system design technique.

CHAPTER 7

ROBUST CONTROL SYSTEM DESIGN OF A FEEDWATER HEATER TRAIN WITH TIME DELAY

In this chapter a level control system is developed for a low-pressure feedwater heater train with time delay using the modified LQG/LTR design and analysis technique outlined in the previous chapter. This application will demonstrate that modern control and analysis techniques are very useful in obtaining a stable control system design for a plant with time delay, thus demonstrating that the process control industry can benefit just as much as the high tech aerospace industry by using modern control techniques.

7.1 LINEARIZED MODEL AND SYSTEM UNCERTAINTY

The nonlinear mathematical model of the low-pressure feedwater heater train shown in Fig. 8 is obtained using the Modular Modeling System (MMS) [29]. The nonlinear plant is linearized about a nominal operating point, resulting in a state differential equation of the form

$$\dot{x} = Ax(t) + Bu(t)$$

$$y = Cx(t) \tag{7.1}$$

where **A**, **B**, and **C** are system matrices. The linearized model consists of 24 state

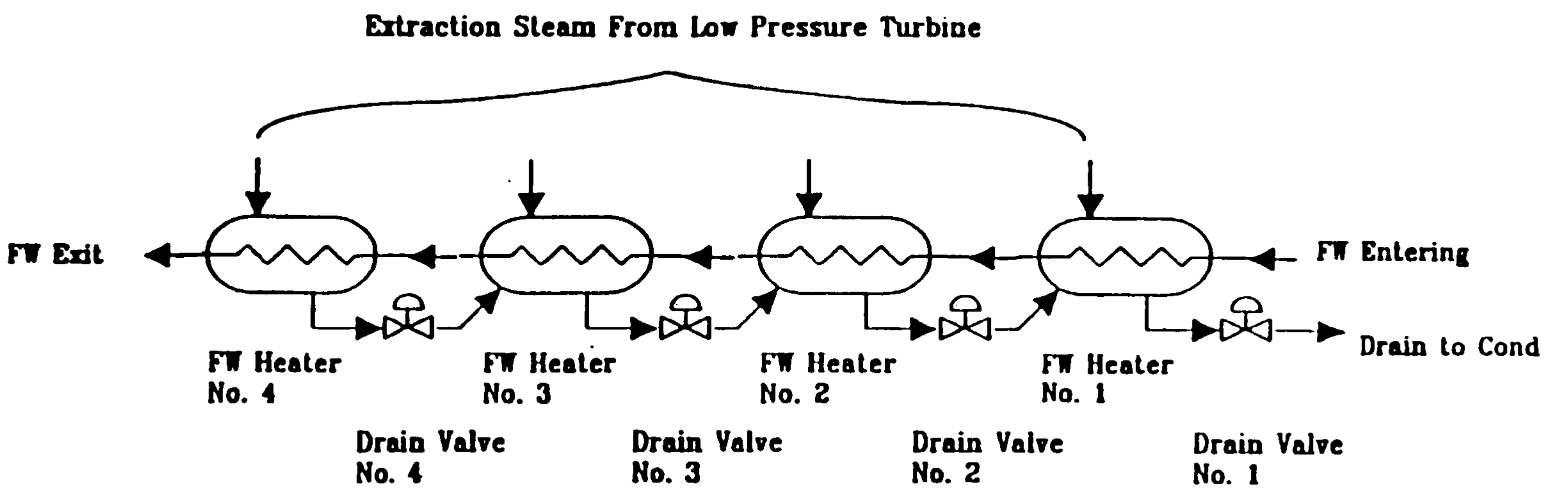

Fig. 8. Flow diagram of low-pressure feedwater heater train.

variables, 4 inputs, and 4 outputs, which are defined in Table 3. The poles and zeros of the linearized plant are shown in Table 4. The system matrices of Eq. (7.1) are used to define the minimum phase model defined in Eq. (6.3).

The time delay in this system will be attributed to computational delay, which is assumed to be caused by the computational limitations of the simulator being used to evaluate the controller. The computational delay is to be 0.5 s. The process dynamics known to be a source of delay in real systems are ignored directly in this design because of a lack of physical realization caused by the use of a lumped-parameter model. Even though no knowledge of process time delay is available during the analysis, the control system's capability to tolerate time delay (which is significantly greater than the computational time delay) will be evaluated.

The time delay system state equations of $B_z(s)$, the output perturbation, are defined using Eqs. (6.6) and (6.7) where $p = 4$ and $\tau_{ii} = 0.5$. The time delay is assumed to vary uniformly in all channels of the plant output. The output multiplicative model uncertainty $\Delta G_D(s)$ due to the time delay is defined as

$$\Delta G_D(s) = \mathbf{I} - B_z(s)$$

Table 3. Low pressure feedwater heater state variables, control inputs and outputs

Order	Descriptions
	State variables - x
1.	Drain cooler exit enthalpy on shell side for FW heater 1 (BTU/lbm)
2.	Drain cooler exit enthalpy on shell side for FW heater 2 (BTU/lbm)
3.	Drain cooler exit enthalpy on shell side for FW heater 3 (BTU/lbm)
4.	Drain cooler exit enthalpy on shell side for FW heater 4 (BTU/lbm)
5.	Inlet pressure on tube side for FW heater 1 (PSIA)
6.	Inlet pressure on tube side for FW heater 2 (PSIA)
7.	Inlet pressure on tube side for FW heater 3 (PSIA)
8.	Inlet pressure on tube side for FW heater 4 (PSIA)
9.	Steam pressure on shell side for FW heater 1 (PSIA)
10.	Steam pressure on shell side for FW heater 2 (PSIA)
11.	Steam pressure on shell side for FW heater 3 (PSIA)
12.	Steam pressure on shell side for FW heater 4 (PSIA)
13.	Condensing region enthalpy on tube side for FW heater 1 (BTU/lbm)
14.	Condensing region enthalpy on tube side for FW heater 2 (BTU/lbm)
15.	Condensing region enthalpy on tube side for FW heater 3 (BTU/lbm)
16.	Condensing region enthalpy on tube side for FW heater 4 (BTU/lbm)
17.	Drain cooler exit enthalpy on tube side for FW heater 1 (BTU/lbm)
18.	Drain cooler exit enthalpy on tube side for FW heater 2 (BTU/lbm)
19.	Drain cooler exit enthalpy on tube side for FW heater 3 (BTU/lbm)
20.	Drain cooler exit enthalpy on tube side for FW heater 4 (BTU/lbm)
21.	Condensing region enthalpy on shell side for FW heater 1 (BTU/lbm)
22.	Condensing region enthalpy on shell side for FW heater 2 (BTU/lbm)
23.	Condensing region enthalpy on shell side for FW heater 3 (BTU/lbm)
24.	Condensing region enthalpy on shell side for FW heater 4 (BTU/lbm)
	Control inputs- u
1.	Drain valve position demand for FW heater 1 (fraction open)
2.	Drain valve position demand for FW heater 2 (fraction open)
3.	Drain valve position demand for FW heater 3 (fraction open)
4.	Drain valve position demand for FW heater 4 (fraction open)
	Outputs- y
1.	Level for FW heater 1 (inches)
2.	Level for FW heater 2 (inches)
3.	Level for FW heater 3 (inches)
4.	Level for FW heater 4 (inches)

Table 4. Plant poles and zeros

Poles		Zeros	
(1)	-288.305	(1)	-176.505
(2)	-176.505	(2)	-288.305
(3)	-63.226	(3)	-63.226
(4)	-5.829	(4)	-4.896
(5)	-4.963	(5)	-5.829
(6)	-3.969	(6)	-3.945
(7)	-2.231	(7)	-2.269
(8)	-1.219	(8)	-1.218
(9)	-0.912	(9)	-0.906
(10)	-0.609	(10)	-0.596
(11)	-0.589	(11)	-0.610
(12)	-0.243	(12)	-0.243
(13)	-0.198	(13)	-0.200
(14)	-0.148	(14)	-2.933e-02 + j1.582e-03
(15)	-0.128	(15)	-2.933e-02 - j1.582e-03
(16)	-0.112	(16)	-4.612e-02
(17)	-7.293e-02	(17)	-7.039e-02
(18)	-4.983e-02	(18)	-0.101
(19)	-3.065e-02	(19)	-0.130
(20)	-2.438e-02	(20)	-0.148
(21)	-2.017e-03		
(22)	-2.558e-04		
(23)	-5.657e-05		
(24)	-2.726e-05		

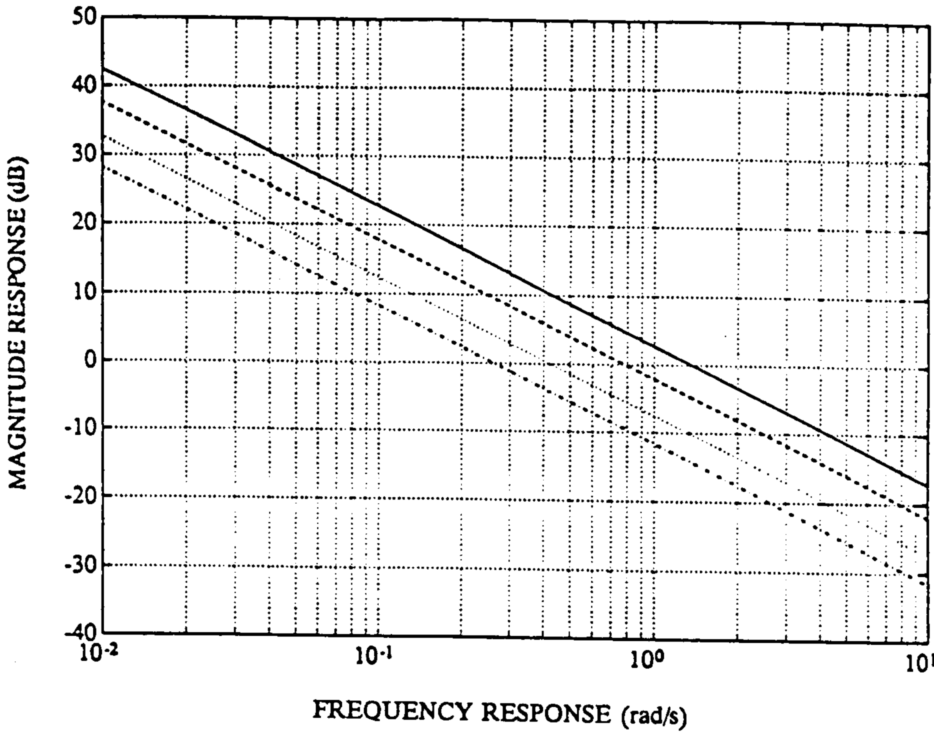

Fig. 9. SVP return ratio of nominal plant $[G(s)]$.

$$\Delta G_D(s) = \begin{bmatrix} \dfrac{-\tau_{11}s}{\tau_{11}s + 1} & 0 & 0 & 0 \\ 0 & \dfrac{-\tau_{22}s}{\tau_{22}s + 1} & 0 & 0 \\ 0 & 0 & \dfrac{-\tau_{33}s}{\tau_{33}s + 1} & 0 \\ 0 & 0 & 0 & \dfrac{-\tau_{44}s}{\tau_{44}s + 1} \end{bmatrix} \tag{7.2}$$

where $\tau_{11} = \tau_{22} = \tau_{33} = \tau_{44} = \tau_{55}$.

7.2 CONTROLLER DESIGN AND EVALUATION

This control system design will require a small or zero steady state output tracking error in response to a required command for a desired feedwater heater tank level. For zero steady state error it requires the control system to add integral action at the plant input if zero steady state error is desired, or the plant to inherently have pure integral action (poles at the origin of the s-plane). As seen from Table 4, the nominal plant under consideration has poles near zero, thus indicating that the system may have some inherent near-integral action. Even though poles and zeros of a plant are useful in assessing the dynamics of a plant, a more useful tool for both SISO and MIMO systems is the singular-value plot (SVP) of the return ratio of the plant (see Fig. 9). This SVP shows that the plant exhibits an integral type of action, deviating from the actual integral SVP by scaler magnitudes over the frequency range shown on the SVP. It appears that by taking advantage of the inherent integral action of the plant caused by certain poles being close to the origin of the s-plane, augmentation of the plant input with integralscan be avoided. Even though exact integrals do not exist in the plant, the ability of the near-integral action of the plant to yield a small tracking error must be examined after the control system design.

Step 1. Now the necessary balancing transformation matrix L and the scalar gain parameter μ will be selected to obtain the appropriate transfer function loop shape $G_{FOL}(j\omega)$ to meet the desired design specifications for this control system as shown in Table 5. An additional constraint required in this design is to place a bandwidth constraint of 0.1 rad/s on the control system. This bandwidth constraint is required because in actual practice a process control system will have a limited rate of response

Table 5. Feedwater Control System Design Specifications

System Requirements	Range
Good command-following	$\underline{\sigma}[G(j\omega)K(j\omega)] \geq 20\ dB \ \ \forall\ \omega < .01\ rad/s$
Good disturbance rejection	$\underline{\sigma}[G(j\omega)K(j\omega)] \geq 20\ dB \ \ \forall\ \omega < .01\ rad/s$
Good immunity to noise	$\overline{\sigma}[G(j\omega)K(j\omega)] < -5\ dB \ \ \forall\ \omega > 1.0\ rad/s$
Good system response to high-frequency modeling error*	$\underline{\sigma}\left\{I + [G(j\omega)K(j\omega)]^{-1}\right\} > \lVert \Delta G_D(j\omega) \rVert \ \ \forall\ \omega > 0\ rad/s$
Good insensitivity to parameter variations at low frequencies*	$\underline{\sigma}[G(j\omega)K(j\omega)] > 10\ dB \ \ \forall\ \omega < .02\ rad/s$

*Note: The ΔG(jw) indicated corresponds to the applicable multiplicative or additive model uncertainty.

due to plant physical limitations. These physical limitations are much more prevalent in process control applications than in applications such as high performance aircraft or the aerospace industry, where modern control techniques also are used.

It is also desired to have the control loops respond similarly considering the bandwidth limitations. Therefore it is required that $G_{FOL}(j\omega)$ have singular values that are equal to 1 [$\sigma_i(G_{FOL}(j\omega) = 1$] at the gain crossover frequency of 0.1 rad/s. Also, it is desired to have the singular values the same at both low and high frequencies, which will assist in achieving the design specifications.

After considering the design requirements and the alternatives of balancing the singular values at either high frequency ($\omega \rightarrow \infty$) or low frequency ($\omega \rightarrow 0$), it was decided to balance the singular values at an intermediate frequency of 0.1 rad/s. An intermediate frequency for balancing was selected because of the symmetry of the singular values at the desired bandwidth and the frequency range of critical interest for the design specifications. Considering the symmetry of the plant, it became apparent that if the singular values are balanced at an intermediate frequency of 0.1 rad/s, the singular values are also balanced at frequencies above and below this frequency in the region of symmetry.

The balancing transformation L of Eq. (6.11) is obtained using a design tool called CASCADE [30]. The scaler μ (the gain parameter) is selected to be 1.0.

Step 2. Using the numerical values of L and μ obtained in Step 1 from Eqs. (6.14) and (6.15), we obtain the desired Kalman filter transfer function which meets the design specifications. The SVP [31] of the Kalman filter transfer function $G_{KF}(s)$ is shown in Fig. 10.

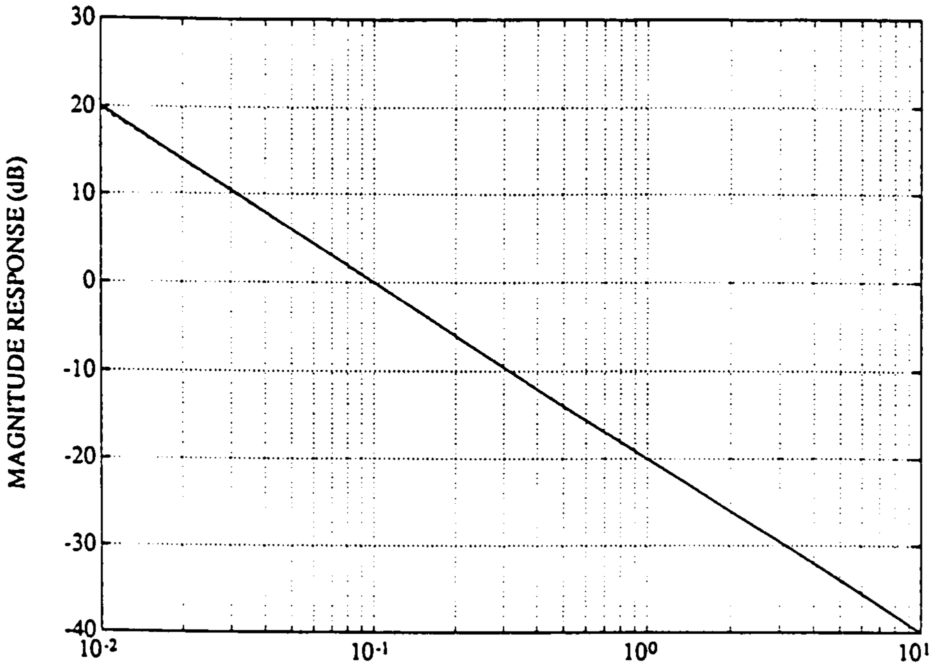

Fig. 10. Singular value plot of the Kalman filter transfer function $[G_{KF}(s)]$.

Step 3. Now it is desired to obtain a numerical value of the regulator gain K such that

$$G(s)K(s) \rightarrow G_{KF}(s) \tag{7.3}$$

or, simply stated, the good performance and robustness stability properties of the Kalman filter are recovered at the plant output. The free design parameter of Eq. (6.18) is selected to be 1.0 in this design. Using CASCADE the numerical value of the regulator gain K is obtained, thus completing the controller design.

The singular-value plots of the return ratio, return difference, and inverse return difference of $G(s)K(s)$ are shown in Figs. 11, 12, and 13 respectively. The SVP of the inverse return difference of $G(s)K(s)$ also includes a plot of the SVP of $\bar{\sigma}[\Delta G_D(s)]$ for $\tau = 0.5$ s. Upon examination of these SVPs it is seen that the desired design specifications are met.

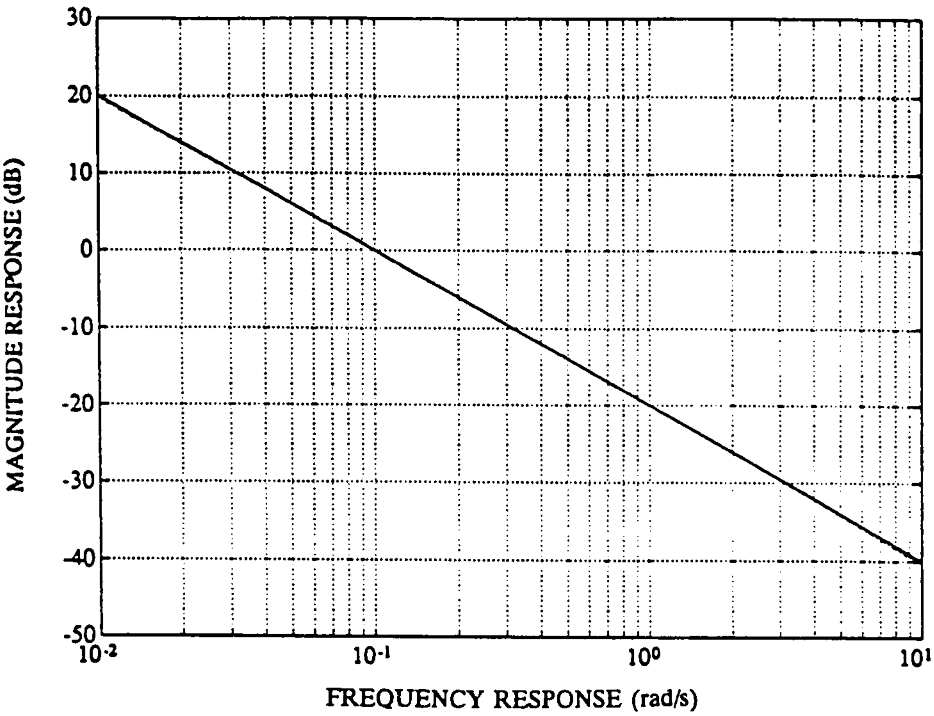

Fig. 11. SVP of the return ratio of a compensated system $[G(s)K(s)]$.

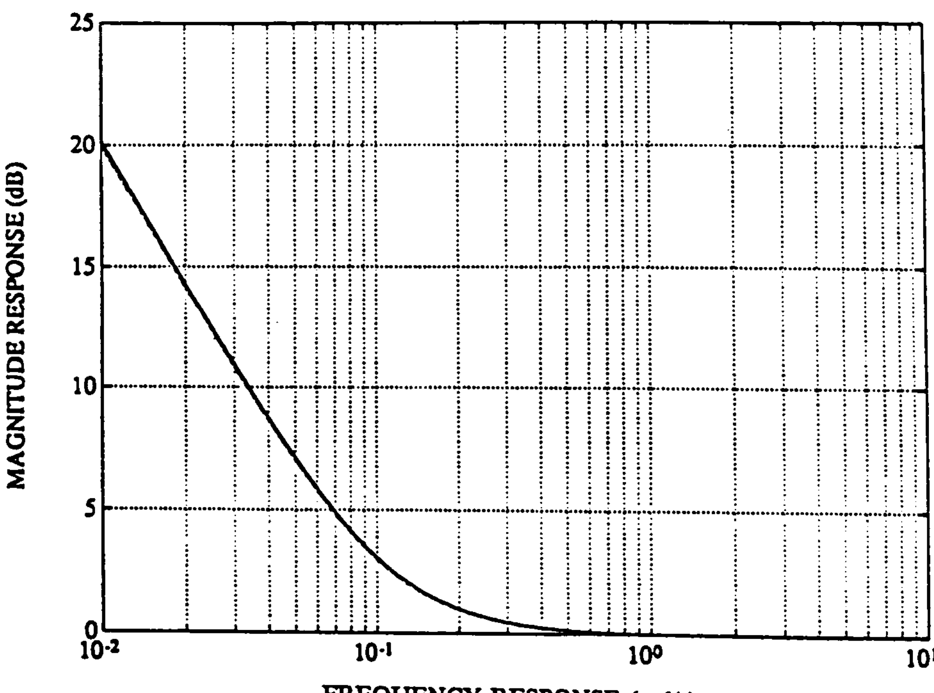

Fig. 12. SVP of the return difference of a compensated system $[I + G(s)K(s)]$.

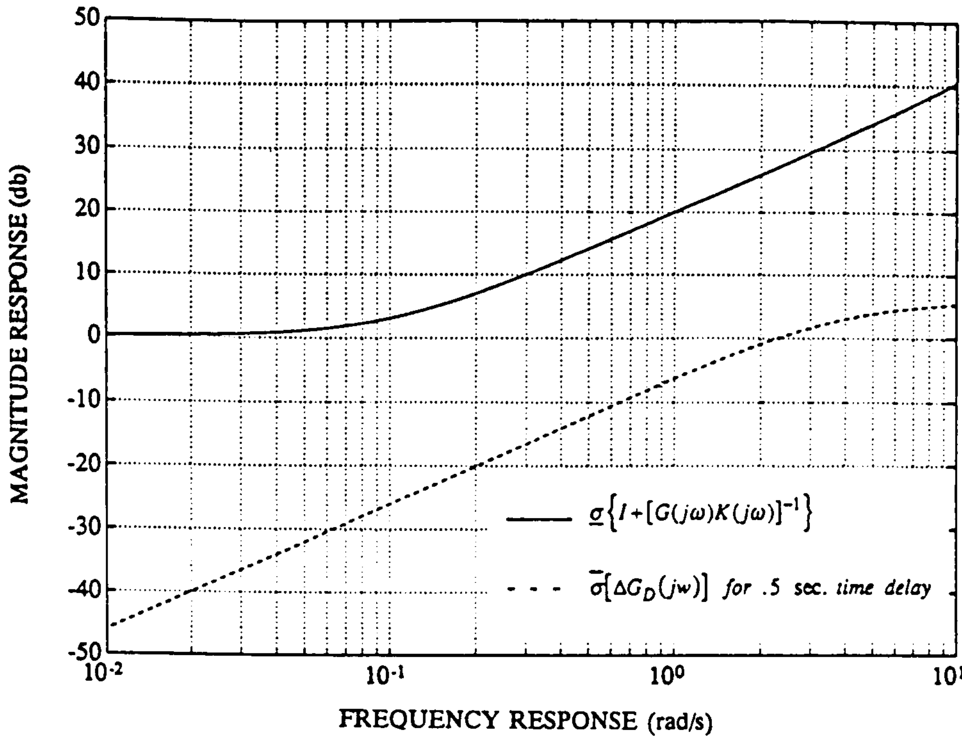

Fig. 13. SVP of the inverse return difference of a compensated system and $\Delta G_D(s)$ for a time delay of 0.5 s.

Step 4. Next the maximum value of allowable time delay that will destabilize the newly designed control system is computed using the analytical method described by Eqs. (4.30) and (4.31). Applying this analytical method yields a maximum allowable time delay (MATD) of τ_A = 14.7 s. Figure 14 shows the SVP of the multiplicative stability bound $\Delta G_D(s)$ with a time delay of 14.7 s and the inverse return difference of the compensated system. It is seen that $\Delta G_D(s)$ for a time delay of 14.7 s is not significant enough to destabilize the compensated system.

As the time delay of $\Delta G_D(s)$ increases above 14.7 s it is seen that the $\bar{\sigma}[\Delta G_D(s)]$ also increases. The amount of maximum time delay, τ_G, that is graphically seen (Fig. 14) to be allowable before the inequality of Eq. (6.22) is ~19.0 s. This graphical result

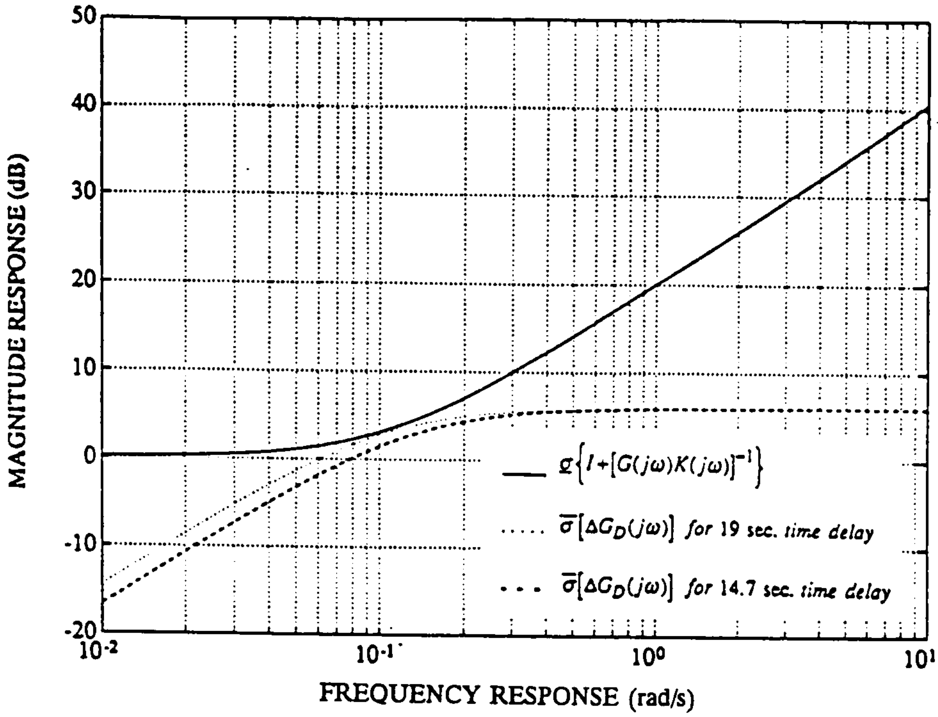

Fig. 14. SVP of the inverse return difference of compensated system and the model uncertainty due to time delays of 14.7 and 19.0 s.

appears to verify that the MATD of τ_A = 14.7 s required to destabilize the control system is a very conservative value.

The output transient responses of the closed-loop level control system are now evaluated as the time delay increases from 0 to 20 s. The transient response of the nominal control system with no time delay is shown in Fig. 15. The results of the transient responses of Figs. 16–18 verify the conservative result of τ_A as the MATD as seen in the frequency domain. The results of Fig. 18 show that the control system becomes unstable at ~20 s, which is slightly greater than τ_G, the graphically obtained value of the MATD required to destabilize the control system.

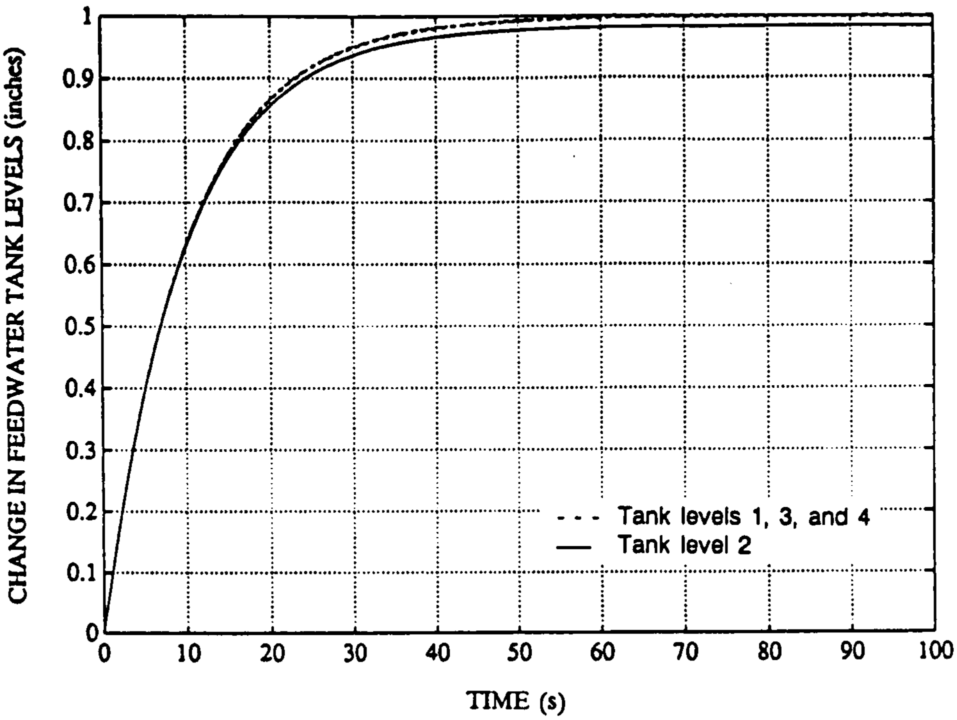

Fig. 15. Transient response for level demand with no time delay.

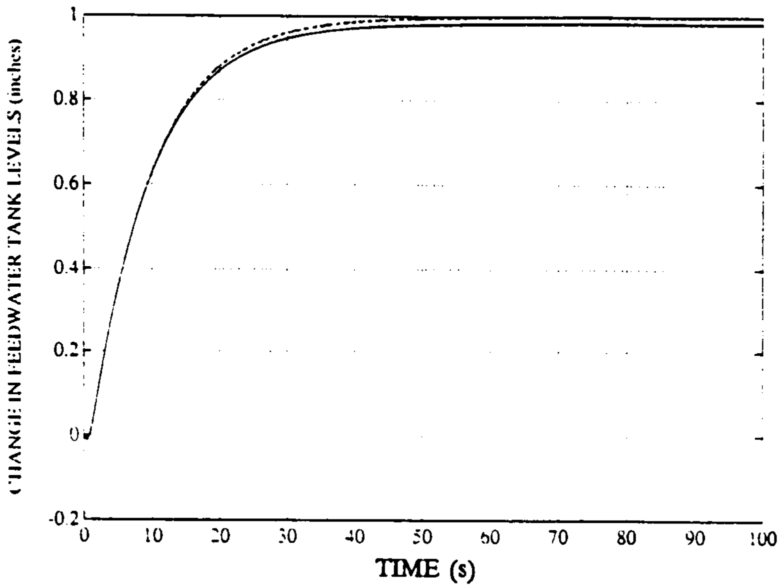

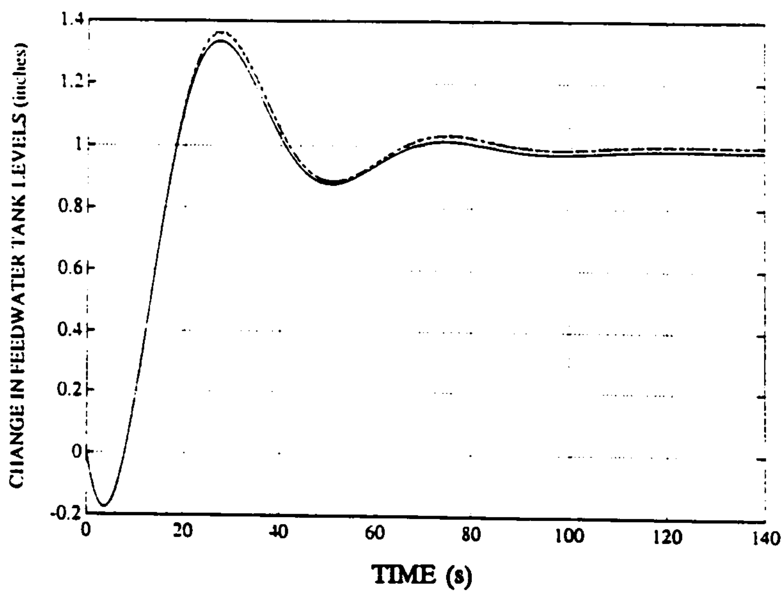

Fig. 16. Transient responses for level demand with time delays of 1.0 and 10.0 s.

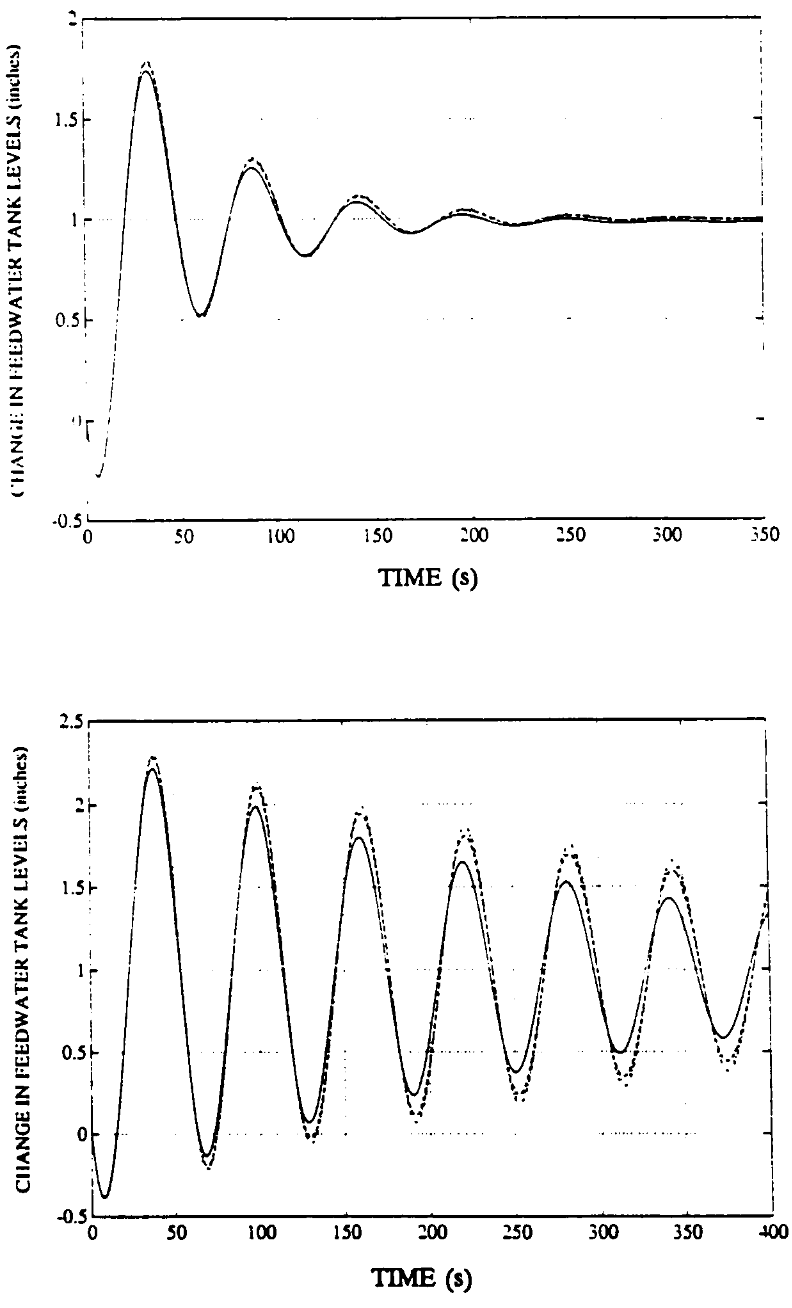

Fig. 17. Transient responses for level demand with time delays of 14.7 and 19.0 s.

Fig. 18.

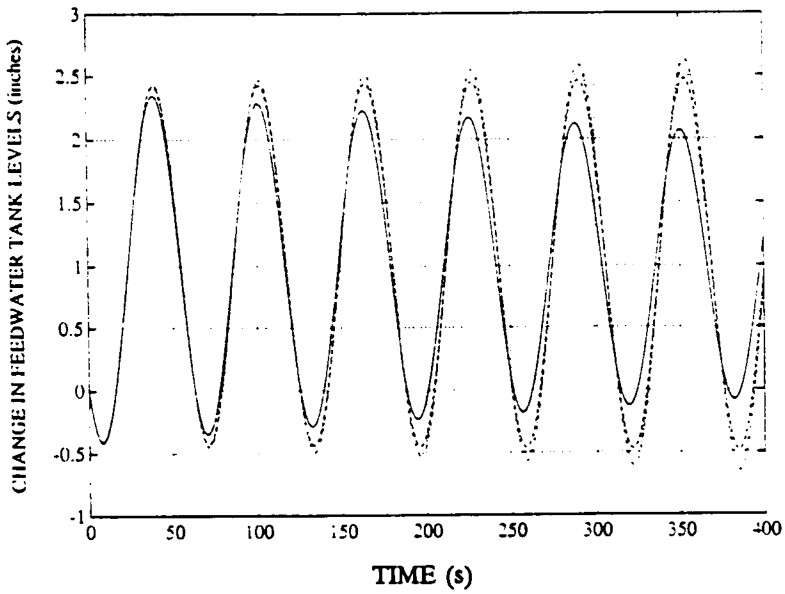

Fig. 18. Transient responses for level demand with a time delay of 20.0 s.

CHAPTER 8

CONCLUSIONS AND RECOMMENDATIONS FOR FURTHER RESEARCH

8.1 CONCLUSIONS

Time delay exists in almost every physical system. In this work the effects of uniformly varied time delay at the plant output are studied.

Achievable performance and stability is sacrificed in the presence of time delay. A linear control system that is closed-loop stable can become unstable when time delay in the plant becomes some significant value. Large time delay results in large overshoots, oscillatory outputs, and initial response action opposite to the desired direction.

The literature has shown that a significant effort has gone into finding solutions to the control system design of plants with pure time delay. The effort to obtain such a control system design presents a formidable mathematical challenge, which has no apparent connection to the widely used classical concepts that allow the control engineer to analyze and specify frequency and time domain specifications more readily.

In this work a systematic control design methodology has been introduced for a system with time delay. The methodology allows the synthesis of a stable control system for plants with uniformly varying time delay at the plant input or output.

In the analysis part, graphical and analytical techniques were presented to evaluate the maximum allowable time delay (MATD) required to destabilize the control system. Through graphical analysis in the frequency domain and time domain analysis the analytical method of computing the MATD is seen to be conservative. The analysis in this methodology allows quick computation of the effects of possible time delay quantities on the stability of an existing or newly designed control system, regardless of whether it is SISO or MIMO.

In the design part of this methodology all of the performance and stability robustness aspects can be established in the frequency domain. The performance robustness of the desired system may be limited by the stability robustness due to noise or model uncertainty, whichever is more restrictive.

The benefit of this methodology is that it allows the synthesis of a stable closed-loop control system with some limitations in achievable performance. Most of all, this methodology allows the classical control concepts for SISO plants with time delay to be used in MIMO plants with time delay, thus avoiding the loss of intuitive control concepts in a vastness of formidable mathematics.

8.2 RECOMMENDATIONS FOR FUTURE RESEARCH

A practical problem of linear control system design involves assuring the stability of the control system in the presence of magnitude and/or rate control saturations. The design of a stable control system for these conditions practically requires obtaining a linear control system design that limits inputs to the plant to an acceptable magnitude and rate of change. The dynamics of input magnitude and rate of change and the resulting output are evaluated in the time domain. However, the time domain characteristics, including stability, are related directly to the frequency response of the singular value plots. It appears that if the linear frequency domain design technique is constrained to provide input control effort that does not saturate the magnitude and rate control bounds dictated by the actuator dynamics, then a stable control system is obtainable. The linear control system design method used could be obtained by augmenting the design steps of the methodology presented in this work, or H_2/H_∞, or μ synthesis control system design methods. In the linear control system design literature there appears little evidence that saturation considerations are part of the design procedure, even in the process control area.

One other area that deserves further research is the application of gain scheduling to process control systems designed using robust control system techniques such as LQG/LTR, H_2/H_∞, and μ synthesis. It appears that there is a void in the literature on the stability and performance of linearly interpolating control gains obtained from control system design at a finite number of nominal operating points. Also, the performance and stability consequences of using a bang-bang approach to gain scheduling for process control applications is an area in which further research is needed.

In this section a few areas of further research that are of practical interest were presented. These areas were mentioned in an effort to establish a tool box of practical control system design considerations including time delay in order to readily facilitate implementation of MIMO robust control design techniques in various areas of industry.

LIST OF REFERENCES

LIST OF REFERENCES

[1] Science Applications International Corporation, "Requirement and Design Specifications of a BWR Digital Feedwater Control System," Electric Power Research Institute report EPRI NP-5502, Project 2448-3, November 1987.

[2] Ray, W. H., *Advanced Process Control*, McGraw Hill, New York, 1981.

[3] Doyle, J. C., "Guaranteed Margins for LQG Regulators," *IEEE Trans. Automatic Control*, vol. AC-23, pp. 756-757, August 1978.

[4] Doyle, J. C., and Stein, G., "Robustness with Observers," *IEEE Trans. Automatic Control*, vol. AC-24, pp. 607-611, August 1979.

[5] Athans, M., "A Tutorial on the LQG/LTR Method," *Proc. American Control Conf.*, Seattle, Wash., June 1986, pp. 1289-1296.

[6] Soliman, M. A., and Ray, W. H., "Optimal Feedback Control for Linear Quadratic Systems Having Time Delays," *Int. J. Control.*, vol. 15, No. 4, pp. 609-627, 1972.

[7] Freudenberg, J. S., and Looze, D. P., "Right Half Plane Poles and Zeros and Design Tradeoffs," *IEEE Trans. Automatic Control*, vol. AC-30, No. 6, pp. 555-565, June 1985.

[8] Doyle, J. C., "Achievable Performance in Multivariable Feedback Systems," *18th IEEE Conference on Decision and Control*, Ft. Lauderdale, Fla., December 12-14, 1979, pp. 250-251.

[9] Morari, M., and Zafiriou, E., *Robust Process Control*, Prentice-Hall, New Jersey, 1989.

[10] Noble, B., and Daniel, J. W., *Applied Linear Algebra*, Prentice-Hall, New Jersey, 1977.

[11] Athans, M., and Falb, P. L., *Optimal Control*, McGraw Hill, New York, 1966.

[12] Stengel, R. F., *Stochastic Optimal Control Theory and Application*, John Wiley and Sons, New York, 1986.

[13] Brogan, W. L., *Modern Control Theory*, Prentice-Hall/Quantum Publishers, 1982.

[14] Takahashi, Y., Rabins, M. J., and Auslander, D. M., *Control and Dynamics Systems*, Addison-Wesley, 1970.

[15] Golub, G. H., and Van Loan, C. F., *Matrix Computations*, John Hopkins University Press, Maryland, 1983.

[16] Cruz, J. B., Jr., Frendenberg, J. S., and Looze, D. P., "A Relationship Between Sensitivity and Stability of Multivariable Feedback Systems," *IEEE Trans. Automatic Control*, vol. AC-26, No. 1, February 1981.

[17] Lehtomaki, N. A., Sandell, N. R., Jr., and Athans, M., "Robustness Results in Linear-Quadratic Gaussian Based Multivariable Control Designs," *IEEE Trans. Automatic Control*, vol. AC-26, No. 1, February 1981.

[18] Doyle, J. C., and Stein, Gunter, "Multivariable Feedback Design: Concepts for a Classical Modern Synthesis," *IEEE Trans. Automatic Control*, vol. AC-26, No. 1, February 1981.

[19] Chen, C. T., *Linear System Theory and Design*, Holt, Rinehart and Winston, New York, 1984.

[20] Friedland, B., *Control System Design*, McGraw-Hill, New York, 1986.

[21] Kazerooni, H., and Narayanan, K., "Loop Shaping Design Related to LQG/LTR for SISO Minimum Phase Plants," *IEEE American Control Conference*, vol. 1, pp. 512-519, June 1987.

[22] Franklin, G. F., Powell, J. D., and Emam-Naeini, A., *Feedback Control of Dynamic Systems*, Addison-Wesley, 1986.

[23] Nesline, F. W., and Zarchan, P., "Why Modern Controllers Can Go Unstable in Practice," *J. Guidance and Control*, vol. 7, No. 4, pp. 495-500, July 1984.

[24] Stevens, B. L., Vesty, P., Heck, B. S., and Lewis, F. L., "Loop Shaping with Output Feedback," *IEEE American Control Conference*, vol. 1, pp. 146-149, 1987.

[25] Doyle, J. C., "Robustness of Multiloop Linear Feedback Systems," *IEEE Conference on Decision and Control*, vol. 1, pp. 12-18, 1978.

[26] Chan, S. M., and Athans, M., "Robustness and Stability of Power-System Models Using Damping and Synchronizing Torques," *20th IEEE Conference on Decision and Control*, San Diego, Calif., December 16-18, 1981, vol. 3, pp. 1203-1211.

[27] Beyer, W. H., *CRC Standard Mathematical Tables*, CRC Press, Inc., 1978.

[28] Birdwell, J. D., and Laub, A. J., "Balanced Singular Values of LQG/LTR Design," *Internat. J. Control*, vol. 45, No. 3, pp. 939-950, March 1987.

[29] Modular Modeling System (MMS), © 1983, Electric Power Research Institute, Palo Alto, Calif.

[30] Birdwell, J. D., Cockett, J. R. B., Bodenheimer, R. E., and Chang, G., *The CASCADE Final Report: Volume II--CASCADE Tools and Knowledge Base*, Electrical Engineering Department, the University of Tennessee–Knoxville, February 19, 1988.

[31] ProMatlab, Version 3.27a, © 1988, The Mathworks Inc., Dearborn, Mass.

APPENDICES

APPENDIX A

REVIEW OF OPTIMAL CONTROL THEORY

APPENDIX A

REVIEW OF OPTIMAL CONTROL THEORY

INTRODUCTION

In the following sections the linear quadratic regulator-based and the Kalman filter-based optimal control problems will be reviewed briefly [A1]. This review will be approached in a manner to set the framework for the study of the LQG and LQG/LTR control system designs.

LINEAR QUADRATIC REGULATOR (LQR)

Consider the linear time-invariant state-space system

$$\dot{x}(t) = Ax(t) + Bu(t) \tag{A.1}$$

where

$$y(t) = Cx(t) \ . \tag{A.2}$$

The goal of this problem is to minimize the performance index

$$J = \int_0^\infty [x^T(t)Qx(t) + u^T(t)Ru(t)]dt + x^T(\infty)Zx(\infty) \tag{A.3}$$

where

$$\int_0^\infty x^T(t)Qx(t)dt = \text{integral square regulating error} \tag{A.4}$$

$$\int_0^\infty u^T(t)Ru(t)dt = \text{integral square input} \tag{A.5}$$

and

$$x^T(\infty)Zx(\infty) = \text{weighted square terminal error.} \tag{A.6}$$

The performance index J, referred to as the quadratic performance index, implies that a control $u(t)$ is sought to facilitate the minimization of J. The weighting matrices Q and R are selected to reflect the importance of particular states and control inputs. In general the weighting of the diagonal elements of Q can be determined by the importance of the state, as observed by the C matrix of the output equation. The effect of Q is the capability to control the transient response of the LQR. The effect of R is to control the energy resulting from u.

A necessary requirement to minimize J is that J is certainly finite. The condition that allows J to become infinite is that uncontrollable, unstable state trajectories appear in the performance index J. Thus the state-space system [A,B] must be completely controllable, or [A,B] must be at least stabilizable to ensure that the performance index is finite.

The control u for the optimization criteria for the steady state linear control law takes the form

$$u(t) = -Kx(t) \tag{A.7}$$

and differentiating Eq. (4.3), it can be shown that S is the solution of the steady state algebraic Riccati equation

$$\dot{S} = 0 = Q - SBR^{-1}B^{T}S + A^{T}S + SA \quad , \tag{A.8}$$

which yields a minimum for the performance index where S, Q, and R are constant positive-definite symmetric matrices,

$$K = R^{-1}B^{T}S \quad . \tag{A.9}$$

At this point the problem of stabilizing the state trajectories appears to be complete, but it is not. What happens when we do not account for unobserved and unstable state trajectories in the performance index of the optimal control law? The result is that the linear controller will not act on the unstable states, thus yielding a finite performance index but an unstable closed-loop system. To eliminate this potential problem, we must required Q to be positive definite, or $Q > 0$. Then the linear control law will yield an asymptotically stable system. Q can be allowed to be positive semidefinite only if [A,C] is observable, where C is a matrix such that $Q = C^T C$ or $C = \sqrt{Q}$. Using

$$Q = C^T C \quad , \tag{A.10}$$

then

$$\begin{aligned} J &= \int_0^\infty [x^T Q x + u^T R u] dt \\ &= \int_0^\infty [x^T C^T C x + u^T R u] dt \\ &= \int_0^\infty [y^T y + u^T R u] dt \quad , \end{aligned} \tag{A.11}$$

which implies that the output system responses are being regulated.

As stated previously, the observability requirement of the pair [A,C] results in a condition sufficient for asymptotic stability of the closed-loop system. This can be made a necessary and sufficient condition by requiring the detectability of the pair [A,C] because only the unstable modes must be moved. Considering the restriction of detectability, the requirement that S be positive definite can be loosened to positive semidefinite.

Using the relaxed conditions, the following summary can be made regarding the linear quadratic regulator (LQR) problem. Given the linear time-invariant plant

$$\dot{x}(t) = Ax(t) + Bu(t) \quad , \tag{A.12}$$

which is stabilizable and controllable, then a finite performance index

$$J = \int_0^\infty [x^T(t)Qx(t) + u^T(t)Ru(t)]dt \tag{A.13}$$

exists, where Q is a symmetric positive semidefinite matrix and R is positive definite. Therefore a linear control law that minimizes J is defined as

$$u(t) = -Kx(t) \tag{A.14}$$

where

$$K = R^{-1}B^TS \tag{A.15}$$

where, in turn, S is a constant symmetric positive semidefinite matrix that satisfies the algebraic Ricatti equation

$$Q - SBR^{-1}B^TS + A^TS + SA = 0 \ . \tag{A.16}$$

The closed-loop regulator is given by

$$\dot{x}(t) = [A - BK]x(t) = [A - BR^{-1}B^TS]x(t) \tag{A.17}$$

and is asymptotically stable provided the state equation (4.1) and the output equation (4.2) are detectable.

KALMAN FILTER

Now we will examine a method of reconstructing an estimate of the states using only the output measurements of the system. The method of reconstruction must be applicable when process noise and measurement noise corrupt the plant state equations and the output measurement equations respectively.

Let us consider the stochastic linear system

$$\dot{x}(t) = Ax(t) + Bu(t) + \Gamma d(t) \tag{A.18}$$

$$y(t) = Cx(t) + n(t) \tag{A.19}$$

where $d(t)$ is a process noise random vector and $n(t)$ is a measurement noise random vector. Assuming that $d(t)$ and $n(t)$ are zero-mean, uncorrelated Guassian white noises, therefore

$$E[d(t)]E[n(t)] = 0 \qquad \text{for all } t \tag{A.20}$$

$$E[d(t)d^T(\tau)] = D_o\delta(t - \tau) \tag{A.21}$$

$$E[n(t)n^T(\tau)] = N\delta(t - \tau) \quad \text{for all } t < \tau \tag{A.22}$$

$$E[d(t)n^T(\tau)] = 0 \tag{A.23}$$

where N and D_o are constant symmetric positive definite and positive semidefinite matrices respectively. Note that N and D_o are constant because it is assumed that $d(t)$ and $n(t)$ are wide-sense stationary.

The state estimate $\hat{x}$ of the state x is obtained from the noisy measurement y. Therefore we can define a state error vector

$$e(t) = x(t) - \hat{x}(t) \tag{A.24}$$

where we desire to minimize the mean square error

$$\bar{e} = E[e^T(t)e(t)] \ . \tag{A.25}$$

The estimator thus can be shown to take the form

$$\dot{\hat{x}} = A\hat{x}(t) + Bu(t) + F[y(t) - Cx(t)] \tag{A.26}$$

where F is the filter gain that minimizes Eq. (4.25); F is defined as

$$F = \Sigma C^T N^{-1} \tag{A.27}$$

where Σ is constant variance matrix of the error $e(t)$. It is assumed here that $e(t)$ is wide-sense stationary. The Σ is obtained by solving the algebraic variance Riccati equation

$$D - \Sigma C^T N^{-1} C\Sigma + A\Sigma + \Sigma A^T = 0 \tag{A.28}$$

where

$$D = \Gamma D_o \Gamma^T \ . \tag{A.29}$$

A condition sufficient to obtain a unique and positive definite Σ from Eq. (4.28) requires that [A,C] be completely observable. However, if the pair [A,C] is required to be detectable then Σ can be positive semidefinite.

The reconstruction error $e(t)$ satisfies the differential equation

$$\dot{e}(t) = [A - FC]e(t) + [\Gamma \ \ -F] \begin{bmatrix} d(t) \\ n(t) \end{bmatrix} \tag{A.30}$$

such that

$$e(t) \rightarrow 0 \ \text{ as} t \rightarrow \infty \ \ \forall t \geq t_o$$

if and only if the observer is asymptotically stable. The poles of the observer (filter) are found using the closed-loop dynamics matrix [A-FC]. To obtain asymptotic stability of the filter, it is required that the pair [A,Γ] be completely controllable. The necessary and sufficient condition of stabilizability of the pair [A,Γ] will ensure stability also.

APPENDIX A REFERENCE

[A1] Kwakernaak, H. and Sivan, R., *Linear Optimal Control Systems*, Wiley-Interscience, New York, 1972.

APPENDIX B

ROBUSTNESS OF FEEDBACK CONTROL SYSTEMS

APPENDIX B

ROBUSTNESS OF FEEDBACK CONTROL SYSTEMS

DEFINITION OF ROBUSTNESS

A system is considered to be robust and have good robustness properties if it has a large stability margin, good disturbance attenuation, and/or low sensitivity to parameter variations [B1]. The term "stability margin" refers to the gain margin and the phase margin, which are quantitative measures of stability. A proven method of obtaining good robustness properties is the use of a feedback control system, which can be designed to allow for variations in the system dynamics. Some causes of variation in system dynamics are as follows:

- modeling and data errors in the nominal plant and system;
- changes in environmental conditions, manufacturing tolerances, wear due to aging, and noncritical material failures; and
- errors due to calibration, installation, and adjustments.

Feedback control systems with good feedback properties have been synthesized for SISO systems. Classical frequency domain techniques such as Nyquist, root-locus, Bode, and Nichols plots have been used to obtain the feedback control system for the SISO system. These design techniques have allowed the synthesis of feedback control systems yielding insensitivity to bounded parameter variations and a large stability margin. The success of the feedback control system for the SISO system has led to the direct extension of the classical frequency domain technique to the design of a multivariable feedback control system. This extension to the multivariable design problem examines an individual feedback loop as the phase and gain margins are varied, while the nominal phase and gain values in the remaining feedback paths are held constant. This technique, however, fails to consider the results of simultaneous variation of gain and phase in all paths, which is a real-world possibility and needs to be considered. A method of obtaining a feedback control system with good robustness properties that takes into consideration simultaneous gain and phase variation is the linear quadratic Guassian (LQG) [B2] technique with loop transfer recovery (LQG/LTR) [B3].

The LQG/LTR technique can be applied to multivariable input/multivariable output (MIMO) systems or SISO systems. The LQG/LTR technique has not only the good robustness properties of the classical frequency domain techniques but also is capable of minimizing the effects of unmodeled high-frequency dynamics, neglected nonlinearities, and a reduced-order model. A tool used in synthesizing the LQG/LTR technique is the computer-aided systems and control analysis and design environment (CASCADE) [B4], an expert computer design tool that eliminates the numerical programming burden of programming the complex LQG/LTR algorithm. The CASCADE expert system was developed for the U.S. Department of Energy by the University of Tennessee at Knoxville.

In this appendix, some concepts will be defined and the LQG/LTR procedure for development of a model-based compensator (MBC) will be described. A unity-feedback MBC is selected for the controller because of its similarity to the SISO unity-feedback control system well known to classical control designers. The MBC closed-loop control system has proven to offer great practical considerations in the design of automatic control systems.

ROBUSTNESS CONCEPTS OF THE LQG AND LQG/LTR CONTROL SYSTEMS

The LQG/LTR [B5] design procedure is based on the system configuration of the LQG controller shown in Fig. B.1. The LQG controller consists of a Kalman filter state estimator and a linear quadratic regulator. The Kalman filter state estimator has been shown to have good robustness properties for plant perturbations at the plant output, and the linear quadratic regulator (LQR) has been shown to have good robustness properties for perturbations at the plant input. Even though its separate components have good robustness properties, however, the LQG controller is found to have no guaranteed robustness properties at either the input (point 2) or the output (point 3) of the plant.

The LQG/LTR design procedure allows us to recover robustness properties at either the input or the output of the plant. If robustness is desired at the input to the plant, first a nominal robust LQR design is made to satisfy the design constraints. Next, an LTR step is made to design a Kalman filter gain that recovers the robustness at the input to the plant of the LQG controller that is approximately that of the nominal LQR design. This implies from Fig. B.1 that the robustness properties at points 1 and 2 are approximately the same.

If robustness is desired at the output of the plant, first a nominal robust Kalman filter design is made to satisfy the performance constraints. Next, an LTR step is made

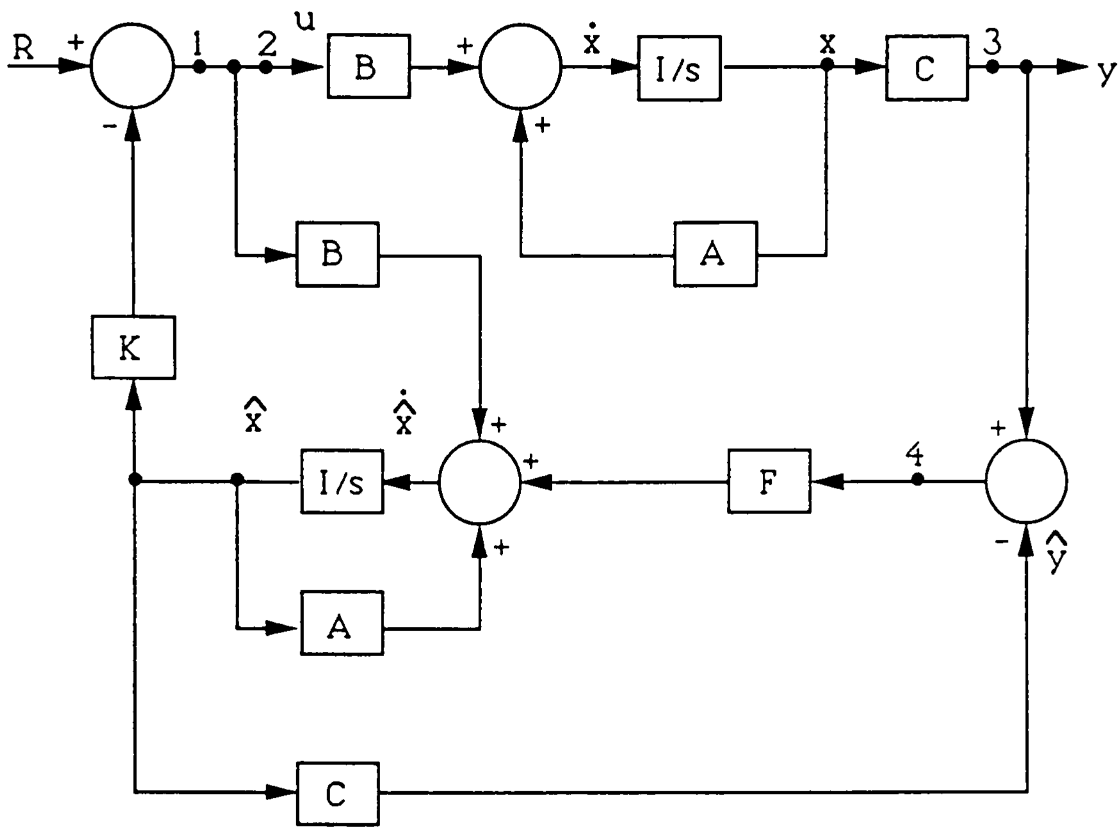

- LQG guaranteed no robustness properties at the input or output of the plant.
- Point 1 has the good robustness properties of the full-state feedback system.
- Point 4 has the good robustness properties of the Kalman filter.
- Point 2 has no guaranteed robustness properties.
- Point 3 has no guaranteed robustness properties.
- the LQG/LTR design method permits recovery of the robustness properties of point 1 at point 2 or the robustness properties of point 4 at point 3.

Fig. B.1. Summary of the robustness properties of the LQG block diagram.

to design a LQR gain that recovers the robustness at the output of the plant that is approximately that of the nominal Kalman filter design. This implies from Fig. B.1 that the robustness properties at points 3 and 4 are approximately the same.

The block diagram of the unity-feedback MBC is shown in Fig. B.2. This control system structure will allow tracking and regulation of a reference input at the output of the plant. The filter and regulator gains used in the controller $K(s)$ are obtained appropriately, depending on whether robustness is desired at the input or the output of the plant. Note that the robustness properties of the unity-feedback MBC (UFMBC) are the same as those of the LQG system because the UFMBC is just an alternate structure of the LQG system.

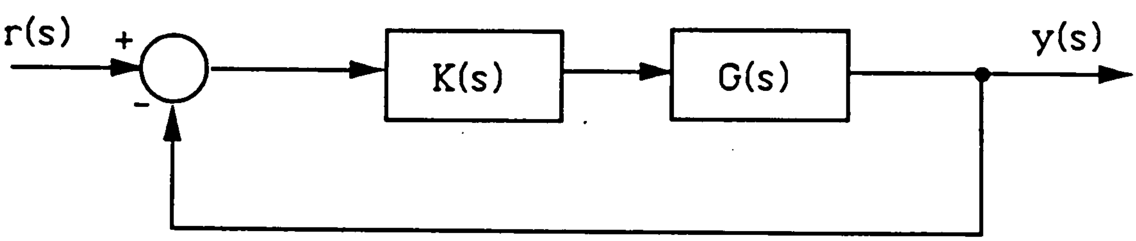

Fig. B.2 Unity feedback model based compensator (UFMBC).

APPENDIX B REFERENCES

[B.1] Safonov, M. G., Laub, A. J., and Hartmann, G. L., "Feedback Properties of Multivariable Systems: The Role and Use of the Return Difference Matrix," *IEEE Trans. Autom. Control*, AC-26, 47-65 (February 1981).

[B.2] Safonov, M. G., and Athans, M., "Gain and Phase Margin for Multiloop LQG Regulators," *IEEE Trans. Autom. Control*, AC-22, 173-179 (April 1977).

[B.3] Stein, G., and Athans, M., "The LQG/LTR Procedure for Multivariable Feedback Control Design," *IEEE Trans. Autom. Control*, AC-32, 105-114 (February 1987).

[B.4] Birdwell, J. D., Cockett, J. R. B., Bodenheimer, R. E., and Chang, G., *The CASCADE Final Report: Volume II--CASCADE Tools and Knowledge Base*, Electrical Engineering Department, The University of Tennessee, Knoxville, February 19, 1988.

[B.5] Kwakernaak, H., and Sivan, R, *Linear Optimal Control Systems*, Wiley-Interscience, New York, 1972.

APPENDIX C

RETURN RATIOS FOR THE FULL-STATE AND OBSERVER-BASED FEEDBACK SYSTEMS

APPENDIX C

RETURN RATIOS FOR THE FULL-STATE AND OBSERVER-BASED FEEDBACK SYSTEMS

FULL-STATE FEEDBACK RETURN RATIO

For the full-state feedback system of Fig. C.1 with no loops broken, it can be stated [C.1] that

$$x = \Phi B u = \Phi B u' \tag{C.1}$$

and

$$u = R - Kx \ . \tag{C.2}$$

Substituting Eq. (C.1) into Eq. (C.2) and solving for u yields

$$u = (I + K\,\Phi B)^{-1} R \ , \tag{C.3}$$

thus

$$x = \Phi B (I + K\Phi B)^{-1} R \ . \tag{C.4}$$

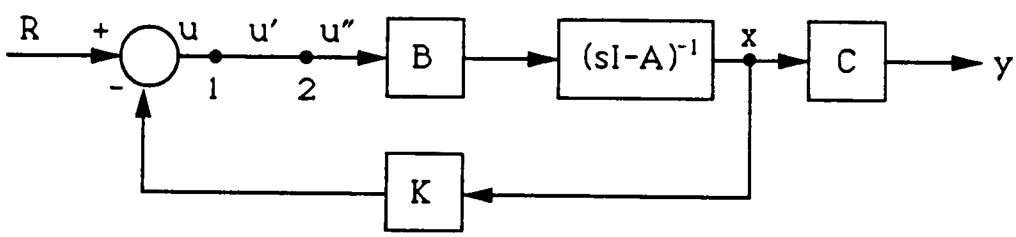

Fig. C.1. Full-state feedback.

Now let us examine the loop transfer function from control signal u' to control signal broken at point 1, assuming that $R = 0$. For this full-state feedback case it follows that

$$x = \Phi B u' \tag{C.5}$$

and

$$u = -Kx \ . \tag{C.6}$$

Substituting Eq. (C.5) into Eq. (C.6) yields

$$u = -K\Phi B u' \ . \tag{C.7}$$

Finally, for the full-state feedback system, find the loop transfer function from control signal u″ when the loop is broken at point 2. In this case it follows that, with $R = 0$,

$$x = \Phi B u'' \tag{C.8}$$

and

$$u = u' = -Kx \ . \tag{C.9}$$

Substituting Eq. (C.8) into Eq. (C.9) yields

$$u = u' = -K\Phi B u'' \ . \tag{C.10}$$

OBSERVER-BASED FEEDBACK RETURN RATIO

For the observer-based feedback system of Fig. C.2 with no loops broken, it follows [C.1] that

$$x = \Phi B u = \Phi B u' = \Phi B u'' \ . \tag{C.11}$$

and

$$y = Cx \ . \tag{C.12}$$

Now substituting Eq. (C.12) and Eq. (C.11) into

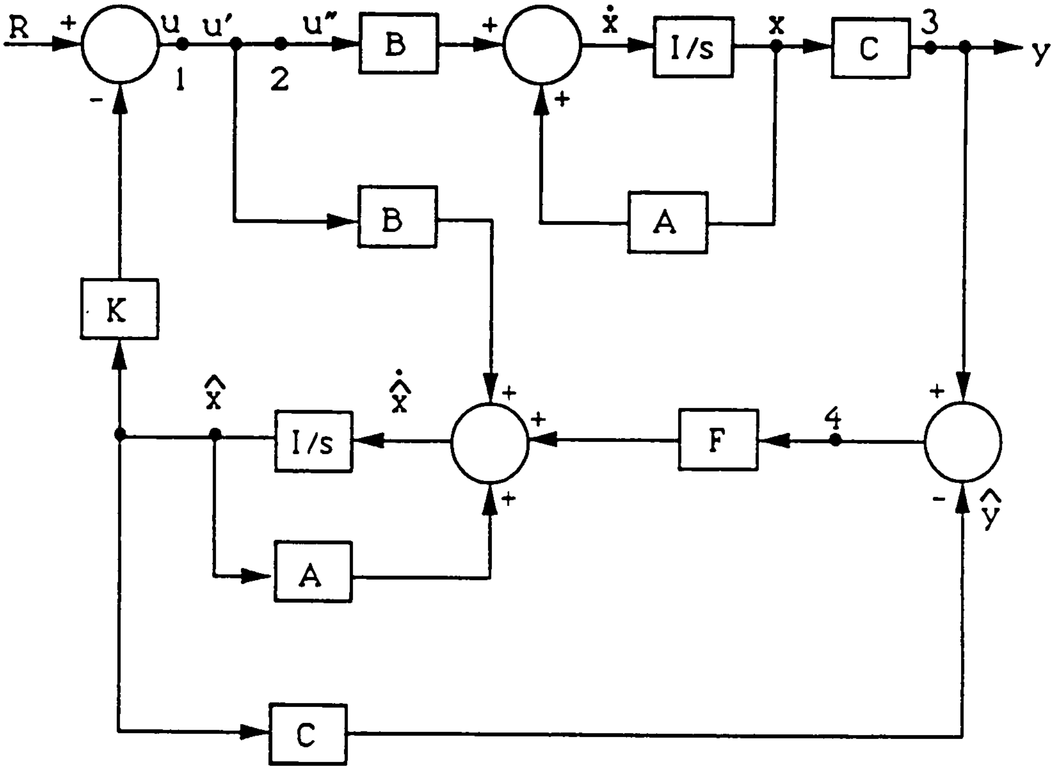

Fig. C.2. Observer-based feedback.

$$\hat{x} = \Phi[Bu' + Fy - FC\hat{x}]$$

results in

$$\hat{x} = \Phi[Bu' + FCx - FC\hat{x}]$$

$$\hat{x} = \Phi[Bu' + FC\Phi Bu' - FC\hat{x}]$$

$$\hat{x} = \Phi[Bu' + FC\Phi Bu'] - \Phi FC\hat{x} \quad , \tag{C.13}$$

thus

$$\hat{x} = (I + \Phi FC)^{-1}\Phi(B + FC\Phi B)u' \quad , \tag{C.14}$$

which simplifies to

$$\hat{x} = \Phi Bu' \quad . \tag{C.15}$$

Now examining the control u, it follows that

$$u = R - K\hat{x} \quad , \tag{C.16}$$

and substituting Eq. (C.15) into Eq. (C.16) results in

$$u = R - K\Phi Bu \quad . \tag{C.17}$$

The control u thus can be defined as

$$u = (I + K\Phi B)^{-1}R \quad . \tag{C.18}$$

Substituting Eq. (C.18) into Eq. (C.11) results in

$$x = \Phi B(I + K\Phi B)^{-1}R \quad , \tag{C.19}$$

which is the same as the result for the full-state feedback system.

Now let us find the loop transfer function from control signal u' to control signal u when the loop is broken at point 1 of the observer-based feedback system. It follows that

$$u = -K\hat{x} \quad , \tag{C.20}$$

and substituting Eq. (C.15) into Eq. (C.20) yields

$$u = -K\Phi Bu' \quad . \tag{C.21}$$

In this case it is clear that $u' = u''$. Also note that the result of Eq. (C.21) is the same as the result found in the full-state feedback case.

Finally, for this observer-based feedback system, the loop transfer function from control signal u'' to control signal u' when the loop is broken at point 2 will be found. For this case

$$\hat{x} = \Phi(Bu' + FC\Phi Bu'') - \Phi FC\hat{x} \quad , \tag{C.22}$$

and solving for $\hat{x}$ results in

$$\hat{x} = (I + \Phi FC)^{-1}\Phi(Bu' + FC\Phi Bu'') \quad . \tag{C.23}$$

Further simplification of Eq. (C.23) results in

$$\hat{x} = \Phi[B(C\Phi B)^{-1} - F(I + C\Phi F)^{-1}]C\Phi Bu' + \Phi[F(I + C\Phi F)^{-1}]C\Phi Bu'' \qquad (C.24)$$

where the plant in this case is square and invertible.

Now the control for this case is defined as

$$u = u' = -K\hat{x} \qquad (C.25)$$

where $\hat{x}$ is defined in Eq. (C.24). This result implies that there is a difference between the control u obtained in Eq. (C.25) for the observer-based feedback system and the control u obtained for the full-state feedback system.

From examination of the loop transfer properties of the full-state feedback system and the observer-based system, it is clear that the input of the observer-based system does not have the good robustness properties of the LQR system. What is now desirable is a means of approximating the loop properties of point 1 at point 2 of the observer-based system.

APPENDIX C REFERENCE

[C.1] Birdwell, J. D., class notes of Modern Control Theory, EE 5291, Electrical Engineering Department, The University of Tennessee, Knoxville, Spring 1986.

APPENDIX D

OBTAINING ROBUSTNESS PROPERTIES AT THE INPUT TO AN OBSERVER-BASED FEEDBACK CONTROL SYSTEM

APPENDIX D

OBTAINING ROBUSTNESS PROPERTIES AT THE INPUT TO AN OBSERVER-BASED FEEDBACK CONTROL SYSTEM

Our previous examination of the observer-based feedback control system commonly referred to as the Linear Quadratic Guassian (LQG) control system showed that there are no guaranteed robustness properties at the input to the plant (point 2 of Fig. C.2). Now a method will be summarized that recovers the good robustness properties of the input (point 2) of the LQR at the input (point 2) of the LQG control system.

Provided that the regulator gain for the LQR has been selected, we must now solve for a filter gain in order to equate the control for the LQG control system for loop break at point 2, which is

$$u = -K\hat{x} \tag{D.1}$$

where

$$\begin{aligned}\hat{x} = {} & \Phi[B(C\Phi B)^{-1} - F(I + C\Phi F)^{-1}]C\Phi Bu' \\ & + \Phi[F(I + C\Phi F)^{-1}]C\Phi Bu''\end{aligned} \tag{D.2}$$

to the control

$$u = -K\Phi Bu'' \tag{D.3}$$

of the LQR for a loop break at point 2. [D.1] To equate the control Eq. (D.1) to the control Eq. (D.3) requires that the following equation be satisfied:

$$B(C\Phi B)^{-1} = F(I + C\Phi F)^{-1} \ . \tag{D.4}$$

Therefore an appropriate value of F must be found to satisfy Eq. (D.4).

Now to select a value of F, we will assume that F is a function of a scalar parameter q such that

$$\frac{F(q)}{q} \rightarrow BW \quad \text{as} \quad q \rightarrow \infty \tag{D.5}$$

where W is any nonsingular matrix. Therefore, using the right-hand sides of Eqs. (D.4) and (D.5),

$$\begin{aligned} F(I + C\Phi F)^{-1} &= \frac{F(q)}{q} q[I + C\Phi F(q)]^{-1} \\ &= \frac{F(q)}{q} \left[\frac{I}{q} + C\Phi \frac{F(q)}{q}\right]^{-1} \quad , \end{aligned} \tag{D.6}$$

which implies that as $q \rightarrow \infty$ Eq. (D.6) becomes

$$BW(C\Phi BW)^{-1} = B(C\Phi B)^{-1} \quad , \tag{D.7}$$

which satisfies the equality requirements of Eq. (D.4) for $W = I$, an identity matrix.

As previously discussed, the error dynamics of the Kalman filter must be asymptotically stable. This requires that an appropriate error noise statistic $\Sigma(q)$ satisfies

$$0 = A\Sigma(q) + \Sigma(q)A^{T} + D(q) - \Sigma(q)C^{T}N^{-T}C\Sigma(q) \tag{D.8}$$

such that

$$F(q) = \Sigma(q)C^{T}N^{-1} \tag{D.9}$$

where $D(q)$ is a positive semidefinite and N is a positive definite, and $[A, D^{1/2}]$ and $[C, A]$ are stabilizable and detectable respectively.

Now $D(q)$, the process noise intensities, and N, the measurement noise intensities, are to be defined respectively as

$$D(q) = \Gamma D_{o}\Gamma^{T} + q^{2}BVB^{T} \tag{D.10}$$

and

$$N = N_{o} \tag{D.11}$$

where $\Gamma = I$, $D_o = C^TC$, and V is any positive definite symmetric matrix.

Substituting Eqs. (D.10) and (D.11) into Eq. (D.8) results in

$$O = A\Sigma(q) + \Sigma(q)A^T + D_o + q^2BVB^T - \Sigma(q)C^TN_o^{-1}C\Sigma(q) \quad , \tag{D.12}$$

which implies that

$$O = A\frac{\Sigma(q)}{q^2} + \frac{\Sigma(q)A^T}{q^2} + \frac{D_o}{q^2} + BVB^T - \frac{\Sigma(q)}{q^2}q^2C^TN_o^{-1}C\frac{\Sigma(q)}{q^2} \quad . \tag{D.13}$$

Now let $q \rightarrow \infty$ in Eq. (D.13); thus

$$q^2\frac{\Sigma(q)}{q^2}C^TN_o^{-1}C\frac{\Sigma(q)}{q^2} \rightarrow BVB^T \quad , \tag{D.14}$$

and using Eq. (D.9), the left-hand side of Eq. (D.14) is then

$$\frac{F(q)N_oF(q)^T}{q^2} = q^2\frac{\Sigma(q)}{q^2}C^TN_o^{-1}C\frac{\Sigma(q)}{q^2} \quad , \tag{D.15}$$

which implies that as $q \rightarrow \infty$

$$\frac{F(q)N_oF(q)^T}{q^2} \rightarrow BVB^T \quad , \tag{D.16}$$

thus

$$\frac{F(q)}{q} \rightarrow BV^{1/2}N_o^{-1/2} \tag{D.17}$$

$$W = V^{1/2}N_o^{-1/2} \quad . \tag{D.18}$$

Thus it can be concluded that as $q \rightarrow \infty$ the loop properties at the input to the plant of the LQG control system approach the input properties of the LQR control system. Note, however, that as $q \rightarrow \infty$ the process noise intensity is seen to differ significantly from the assumed process noise. However, as $q \rightarrow 0$ the Kalman filter is approached.

Thus when $q = 0$ the LQG system has no guaranteed loop properties at the input. It appears that a trade-off must be made between obtaining an accurate filter and obtaining good loop transfer properties.

APPENDIX D REFERENCE

[D.1] Birdwell, J. D., class notes of Modern Control Theory, EE 5291, Electrical Engineering Department, The University of Tennessee, Knoxville, Spring 1986.

VITA

Gregory Vonzell Murphy was born in Memphis, Tennessee, on April 8, 1956. He received his elementary and secondary education in the public school system of Memphis. He entered the University of Tennessee at Knoxville in September 1974 and received a Bachelor of Science in Electrical Engineering in December 1979. He also participated in the University of Tennessee co-operative engineering program while he pursued his undergraduate degree. During his participation in this program he acquired two years of work experience with the Arkansas Operations of the Aluminum Company of America (ALCOA).

From January 1980 to December 1982 he was employed as an electrical engineer at ALCOA's Arkansas Operations. He also pursued part-time graduate studies at the University of Arkansas Graduate Institute of Technology in Little Rock from August 1980 to December 1982. In 1980 he received his Engineering In Training Certificate from the Arkansas State Board of Registration for Professional Engineers.

From December 1982 until September 1984, he was an employee of the Oak Ridge National Laboratory, presently managed by Martin Marietta Energy Systems. He pursued further part time graduate studies in electrical engineering at the University of Tennessee at Knoxville from January 1983 to June 1984. In September 1984 he took a leave of absence from Martin Marietta Energy Systems to pursue full time graduate studies. He received his Master of Science degree in Electrical Engineering in June 1986. He has worked at UTK as a teaching assistant in circuits for over one year and as a research assistant in the area of advanced control system design during the last three years. The research work involves the application and design of robust multivariable control systems.